Journal of Modern Physics, 2023, 14, 461-500
https://www.scirp.org/journal/jmp
ISSN Online: 2153-120X
ISSN Print: 2153-1196

Imagine the World, New Insight into Creation, Gravity and Evolution*

Jarl-Thure Eriksson

Åbo Akademi University, Åbo, Finland
Email: jarl.thure.eriksson@gmail.com

How to cite this paper: Eriksson, J.-T. (2023) Imagine the World, New Insight into Creation, Gravity and Evolution. *Journal of Modern Physics*, **14**, 461-500.
https://doi.org/10.4236/jmp.2023.144027

Received: February 6, 2023
Accepted: March 20, 2023
Published: March 23, 2023

Abstract

Since the publication of Einstein's theory of general relativity, a variety of interpretations have been suggested. In 1937, Paul Dirac presented his Large Number Hypothesis (LNH) based on the large difference between gravitational and electromagnetic forces. As a consequence, the energy is proportional to the radius squared and the gravitational constant is inversely proportional to the radius of the universe. The energy increases during expansion, Dirac used the term "additive creation". The objective is to prove the validity of Dirac's claims. A new theory, CBU (Continuously Breeding Universe), has been developed. The universe is considered a black hole originating from the single fluctuation of a positron-electron pair. The expansion is driven by the formation of new pairs. The negative gravitational potential energy balances the increase in matter energy. Due to $G \sim 1/r$, the Planck length ℓ_p and Planck time t_P depend on the curvature of space. The Schrödinger solution of an initial positron-electron fluctuation contains a parameter equal to the Planck length. The CBU theory postulates that the primordial universe undergoes a transition from a black hole to a photon-filled universe. After the transition, one half of the energy is bound to numerous "small" black holes, the seeds for galaxies, while the other half propagates as CMB (Cosmic Microwave Background) radiation. The CMB photons are due to e^+ - e^- annihilations. Characteristically, the CMB photons are pairwise entangled, the radiation loses wave energy but compensates by increasing the photon numbers. According to a new model for black holes, a continuous inflow of matter prevents the black holes from becoming singularities. An energy gap between the event horizon and the inner photon sphere is the source of real matter from a QED vacuum foam. There is evidence that all stellar matter originates from a proton-antiproton outflow from the galaxy central black hole.

*Die Welt ist alles, was der Fall ist-Ludwig Wittgenstein, Tractatus, 1921. (The World is all that is the case).

Keywords

General Relativity, Gravitation, Black Holes, Singularity, CMB

1. Introduction

Astronomy opens windows to the universe. To understand the physics behind the clockwork of the world, we must use our imagination (Einstein's Gedanken experiment). Step by step, the theory emerges from observations and scientific methodology.

Astronomy has deep roots in history, early observations have been important for the timing of historical events and for the understanding of astrophysical phenomena. However, astronomy as a scientific discipline started with Galileo Galilei at the beginning of the 17th century. The invention of the telescope made it possible to observe the motions of the planets and their moons, giving support to the Copernican heliocentric model.

The accumulation of observational data and the development of tools of increasing sophistication, most recently the Hubble Telescope and the James Webb Space Telescope, have greatly improved our view of the cosmos and its past.

The Big Bang theory, the basis of the present standard model (ΛCDM), was first proposed by the Belgian priest Georges Lemaitre, who used the term "the Primeval Atom" for the Big Bang event [1]. As a religious person, Lemaitre interpreted this as an act of creation, a view that has been accepted by the Vatican and the Catholic Church. Lemaitre also described the expansion of the universe.

The discovery of the cosmic microwave background radiation (CMB) in 1964 has been a key piece of evidence for the Big Bang. Photons following a black body intensity distribution come from all directions of the universe. The spatially even distribution at a time very close to the initial event has been interpreted as very strong argument.

There are several problems related to the standard theory, however. It is assumed that all the energy was packed into the singularity from which the bang started. What was the origin of this energy? To get on track for the coming expansion, the universe had to make a rapid transition from the singularity scale to a scale leading to the current size. One had to introduce inflation, ingeniously developed by Alan Guth [2].

The introduction of dark energy and dark matter, concepts required to explain the expansion and the motions of the celestial bodies, is an extraordinary intervention in science, especially in physics. These concepts are invented just to defend a specific theory, the roots of which are blurred. So far all attempts to find a candidate for dark matter have failed. Dark energy is a trickier question, in this study we will present a solution based on quantum mechanics, which will give a plausible explanation to the dark energy concept.

In the standard model, there is no theoretical derivation or equation for the Hubble constant de facto a time dependent parameter (Edwin Hubble made his observations of the expanding universe in 1923, but only published in 1929 [3]). For practical reasons astronomers use a statistical formula, where the components of matter (dark matter included), dark energy and radiation are fitted in. Here we derive an equation that yields a result 0.5% from observations.

In 1916, Albert Einstein published the Theory of General Relativity (GR) [4]. The theory has formed the backbone of our understanding of gravity. Time and time again, the theory has been proven correct. Einstein's field equation combines the geometry of the universe with energy and momentum. Gravity is explained as a result of the curvature of space. Energy bound to matter or electromagnetic radiation follows a geodesic line as it travels through space. In the empty space around a point-like mass, the ultimate geodesic line coincides with the arc of the radius of curvature. In reality, near celestial bodies, the curvature is distorted.

There were many things that Einstein did not know when he formulated his equations. For instance, the expansion of the universe was still hidden in the veil of the unknown. Not to mention an accelerated expansion. The theory at the time was an unchanging steady state universe. To Einstein Newton's gravitational constant G was a physical fact needed to describe the special case of Newtonian gravitation.

But there was a problem that bothered him, the field equation was unstable, it required an extra term to fulfill the steady state condition. Less than a year after the publication of the GR theory Einstein introduced the idea of a cosmological constant, [5]. Later he would call this as his biggest blunder. This remark received great publicity; it was hard to believe that a genius should admit a mistake. However, the article was not that bad. Much later the cosmological constant was reintroduced to explain the expansion. In the cosmological constant article Einstein defines the curvature radius R_E, also called the Einstein radius, which appears to be close to the present estimate of the radius of the observable universe. The radius is $R_E = c/\sqrt{4\pi G\rho} = 4.6\times10^{26}\ \text{m}$, which should be compared to $R_\Lambda = 4.4 \times 10^{26}$ m (the standard model). Here, the density of real matter was taken to $5 \times 10^{-28}\ \text{kg/m}^3$, a representative value.

Einstein also estimated the total mass by multiplying the density by the volume $V = 2\pi^2 R_E^3$, which is a 4d surface projected into 3d. It is also the volume of a horn torus, **Figure 1(a)**. By using this choice, Einstein sought a 3d shape that would illustrate how light circulates throughout the universe and returns to the point of origin.

In this study, we will stick to Einstein's field equation and interpret the geometry as the interior of a 4d black hole (*BH*). It is impossible to imagine a 4d configuration without an outer surface and without a centre. Instead, we use a 3d projection as shown in **Figure 1(b)**. This assumption leads to solutions that eliminate some problems with the standard model. The *universe BH* has a very

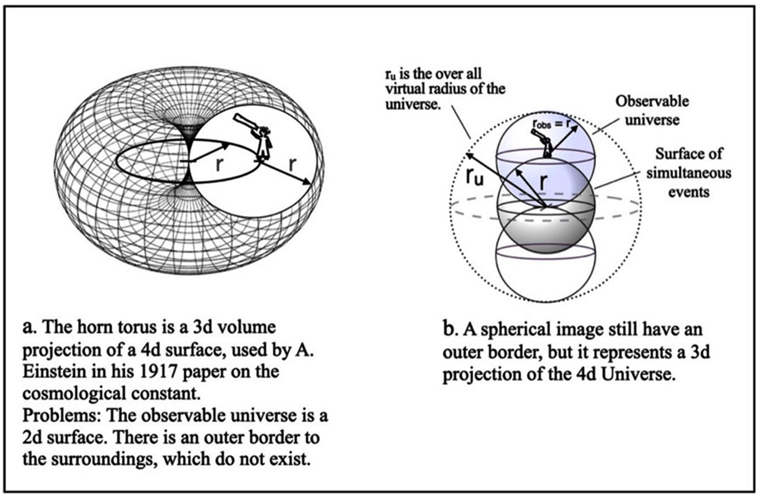

Figure 1. Geometric 3d interpretations of a 4d black hole universe.

low energy density. A steady addition of matter, electrons and positrons, say, prevents a contraction and the formation of a singularity. The influx is a quantum mechanical process made possible by a "momentum-space window" in accordance with the Heisenberg uncertainty principle. The energy of the new matter is balanced by the growth of space and an increase in the gravitational negative potential energy. This important principle was proposed by Alan Guth in an Appendix to [2].

By introducing an acceleration parameter B, we can define the pressures responsible for the expansion, all of which can be formulated as functions of B: Eulerian pressure (introduced by Einstein), a momentum change pressure caused by the influx of new matter, and the pressure responsible for the acceleration. The last-mentioned component is linked to an intrinsic acceleration of space expansion giving rise to a Coriolis effect, which in turn eliminates the need for dark matter.

The most speculative suggestions are omitted. These are inflation, dark matter, singularities, wormholes and the multiverse. We do not deny their existence but do not find them necessary for this study. Though, the theory requires two bold postulates:

1) The CMB radiation is the result of a transition, where the primordial black hole universe releases 50% of its energy as photons from electron-positron annihilations and agglomerates the rest of the energy as matter into a vast array of black holes, the seeds for future galaxies.

2) All stellar matter is the product of proton and antiproton excitations from the event horizon of the galaxy's central black hole.

The study is based on a theory developed by the author in a series of publications during 2018-2022, [6]-[11]. The theory is called CBU, which stands for the Continuously Breeding Universe. The goal is to prove that the CBU theory obeys known laws of physics, the predictions agree with observations and the applied physics proves that the postulates are credible and not coincidences.

2. The Black Hole Universe

The principle that a celestial body possesses such gravity that even light cannot escape was first proposed by the French mathematician Pierre-Simon Laplace and the English physicist John Michell in the late 18th century. A modern approach was implemented by the German mathematician Karl Schwarzschild in 1916, right after the publication of the GR theory. He was the first person to present a solution to the Einstein Field Equation by creating his own metric and deriving the Schwarzschild radius, *i.e.* the radius of the event horizon of a black hole.

Major theoretical work has been going on since the 60s. Stephen Hawking and Roger Penrose became well known for their work on black hole entropy, Hawking radiation and the singularity problem. Some attempts to describe the universe as a black hole have been made, most on purely theoretical grounds, without being able to produce testable predictions. The first serious suggestion to a black hole universe was published by R. K. Pathria in 1972, [12]. The question then—as well as today—was "is the universe closed or open?" By postulating a closed universe Pathria saw a possibility to find explanations to observations of distant phenomena. He proclaims: "Here I demonstrate that the universe may not only be a closed structure but may also be a black hole, confined to a localized region of space which cannot expand without limit."

In 2013, Bernard McBryan published a comprehensive analysis of alternative geometrical solutions for black holes, [13]. He used various metrics as proposed by theorists in previous years. In conclusion he states that one could live in a low-density black hole without really knowing it. But in his study the gravitational parameter G is kept constant. We are going to show that this is not consistent with a black hole universe.

The current study differs from previous attempts in a radical way, the black hole is a main actor in the celestial interplay between time, space and energy. The quantum mechanical activity across the characteristic boundaries, the event horizon, $r_s = 2GM/c^2$ (Schwarzschild radius), and the real black hole radius (the inner photon radius) $r_B = GM/c^2$, makes the black hole's vicinity a cauldron of tumultuous creation. M is the total internal energy in mass units.

The Heisenberg uncertainty principle allows virtual particles from a vacuum ground state to become real not by creating new energy but by balancing the addition of matter with an increasing portion of negative potential energy due to gravitation.

This is the explanation for gravity. The growth of matter requires an expansion of space to increase the negative energy. Thus, the radius of curvature r becomes a measure of gravity. A parameter G, inversely proportional to r, is a convenient way to estimate the gravitational force at a specific time and for a specific size of the universe.

We must make a distinction between the universe black hole and the black holes in the centres of the galaxies. Often the former is described as a cocoon, the surface of a sphere expanding like the universe, without a centre, however, we are on the inside. The universe includes everything: space, time, matter and radiation. Einstein's theory of General Relativity is about the 4d geometry of a black hole and the interpretation that the curved space is an indication of the gravitational effect. The Einstein Field Equation joins geometry with the content of energy and momentum.

The black holes in the centres of galaxies should be treated as spherical cosmological objects, the properties of which have so far remained mysterious. By interpreting the observations made and accepting the postulate of matter influx, we can create a more accurate picture of the black holes and their physical behaviour. A common characteristic of both the *universe* BH and the *galaxy* BH is that they are not singularities. They are dynamic objects that grow by letting streams of elementary particles enter the interior space. The *universe BH* expands, while the *galaxy BH* increases its density.

3. Basic Equations and Geometry

The official view of a black hole is incomplete. On the one hand, it has a mass, a temperature and an entropy, on the other hand, it is just a dive of the fabric of space into an infinitely deep well, the singularity. We claim that this description is inconsistent and incorrect. The black hole contains energy in the form of matter and radiation. The outer surface of the black hole has a distinct radius, half the Schwarzschild radius. We have called this limit the inner photon sphere, it is motivated by the fact that the ultimate photon energy required to escape the BH is $hf = GMhf/(r_B c^2)$, h is the Planck constant and f is the radiation frequency, from which we have the BH radius

$$r_B = \frac{GM}{c^2}. \tag{1}$$

Here G is the gravitational parameter and M the mass of the black hole. Instead of hf we could put any mass energy mc^2 and obtain the same radius. We can also interpret r_B as the distance from a mass centre M required to create a particle m.

Postulating that the universe is a black hole means that Equation (1) also is valid for the universe. The limit for our range is also the radius of the universe:

$$r_u = \frac{r_s}{2} = \frac{GM_u}{c^2}. \tag{2}$$

Here M_u is the total energy of the universe in mass units. Equation (2) is familiar from several significant proposals, most important those by Brans and Dicke [14] and Dirac [15]. For practical reasons we introduce

$$r = \frac{r_u}{2} = \frac{GM_u}{2c^2}. \tag{3}$$

Later we will show that r equals the radius of the observable universe and the Einsteinian curvature radius.

Figure 1(b) visualizes the 3d projection of the 4d universe black hole. The interpretation is relevant as we will see throughout this analysis. The volume and surface of the 3d projection are

$$V_u = \frac{32\pi r^3}{3}, \tag{4}$$

$$A_u = 16\pi r^2. \tag{5}$$

From Equation (3) we have

$$\frac{G}{r} = \frac{2c^4}{W_u}, \tag{6}$$

where $W_u = M_u c^2$ is the total energy, matter and radiation, of the universe.

The first electron-positron pair appears at the initial event, at which point the following condition is satisfied

$$\frac{G_i}{r_i} = \frac{2c^2}{2m_e} = \frac{c^2}{m_e}, \tag{7}$$

Here G_i is the initial gravitational parameter, r_i is the radius and m_e the electron rest mass. The radius is calculated by forming the energy balance equation, Figure 2. The distance between the particles is obtained by multiplying with π: πr_i.

The energy equation is

$$2m_e c^2 = G_i \frac{m_e^2}{\pi r_i} + \frac{e^2}{4\pi\varepsilon_0 (\pi r_i)}, \tag{8}$$

where e is the electron charge and ε_0 is the vacuum permittivity. From Equation (8) we obtain the initial radius

$$r_i = \frac{e^2}{4\pi\varepsilon_0 m_e c^2 (2\pi - 1)}. \tag{9}$$

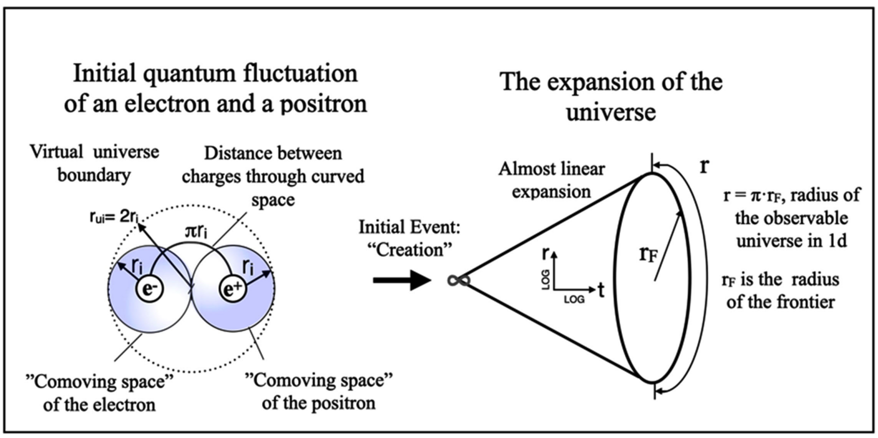

Figure 2. A description of the Genesis event and schematically the expanding universe as the 2d surface of the cone figure. The radius of the observable universe equals πr_F, where r_F is the radius of the frontier circumference (the same presentation as used by NASA, cf. Figure 6).

The value is $r_i = 0.53337905 \times 10^{-15}$ m. It will be shown later that the radius r_i is a fundamental cosmological quantity.

In [9] it was demonstrated that the following relation is valid

$$G_i r_i = Gr = \frac{r_i^2 c^4}{W_e} = constant. \tag{10}$$

As the present value of the Newton gravitational parameter is known, $G_0 = 6.6743015 \times 10^{-11}$ N·m^2/kg^2, we obtain the radius of the observable universe

$$r_0 = \frac{1}{G_0} \cdot \frac{r_i^2 c^4}{W_e} = 4.20550 \times 10^{26} \text{ m}. \tag{11}$$

The value differs from the official figure of 4.4×10^{26} m by −4.6%, a small discrepancy considering the uncertainties in the estimation chain. When G_0 from Equation (11) is substituted into Equation (6), we have

$$W_{u0} = 2W_e \left(\frac{r_0}{r_i}\right)^2 = 1.018 \times 10^{71} \text{ J} \sim 1.133 \times 10^{54} \text{ kg}. \tag{12}$$

The value in kg divided by 8 (the observable universe), $M_{uobs} = 1.42 \times 10^{53}$ kg, matches almost exactly the estimate given by Wikipedia/Observable Universe: $M_{uobs} = 1.46 \times 10^{53}$ kg.

Equation (12) proves that the real energy content is proportional to r^2. The author has defined the following definition

$$W_u = 4\pi b r^2. \tag{13}$$

Here b is a universal energy "pressure" constant, J/m^2, which is obtained from the initial event conditions

$$b = \frac{2W_e}{4\pi r_i^2} = 0.458017 \times 10^{17} \text{ J/m}^2. \tag{14}$$

There are some equations that are of vital importance for the study. The gravitational parameter is

$$G(r) = \frac{c^4}{2\pi b r}. \tag{15}$$

The density of matter (m) and radiation (x) is obtained from

$$\rho_{mx} = \frac{W_u}{V_u c^2} = \frac{3b}{8rc^2}. \tag{16}$$

In his original text on GR Albert Einstein introduces the Eulerian hydrodynamic pressure P_E, capital P is used for pressure to distinguish it from momentum p. From basic thermodynamical principles we have $\mathrm{d}W_u = -P_E \mathrm{d}V_u$. We differentiate the energy relation of Equation (13) and obtain $\mathrm{d}W_u = 8\pi br \cdot \mathrm{d}r = -P_E \mathrm{d}V_u$, then by substituting $dV_u/\mathrm{d}r = 32\pi r^2$ we have

$$P_E = -\frac{b}{4r}. \tag{17}$$

The ingredients needed for a deeper exploration of the dynamic behaviour of the universe are now at hand.

4. The Expanding Universe

4.1. Acceleration

The first observations of an accelerated expansion of the universe were made in the late 1990ies by two independent groups, cf. [16]. The result is significant, because it implies that either there is an unknown form of energy (dark energy) involved or the influx of new matter causes the rate change. Actually, both approaches may be compatible, a virtual quantum ground state energy provides the source of a particle influx. The theoretical dark energy is an integrated rating of the instantaneous ground state values. It is important to determine an approximation of the acceleration, even if there does not exist a purely mathematical solution.

The Einstein Field Equation in its original form is

$$G_{\mu\nu} = 8\pi G T_{\mu\nu}, \tag{18}$$

where $G_{\mu\nu}$ is the Einstein tensor and $T_{\mu\nu}$ is the energy-momentum tensor. The Friedmann solution in Robertson-Walker metrics is, cf. [17],

$$\left(\frac{\dot{a}}{a}\right)^2 = \frac{8\pi G\rho}{3} - \frac{kc^2}{\left(ar_{cur0}\right)^2}. \tag{19}$$

Here a is the scale factor, such that $r = ar_0$, and r_{cur} is the curvature radius. The curvature factor k is −1, 0, +1 for negative, zero and positive curvature respectively.

We derivate Equation (19) with respect to time

$$2\dot{a}\ddot{a} = \frac{8\pi}{3}\left(Ga^2\dot{\rho} + 2G\rho a\dot{a} + \dot{G}\rho a^2\right). \tag{20}$$

We have

$$\frac{\ddot{a}}{a} = \frac{4\pi G}{3}\left(\frac{a}{\dot{a}}\dot{\rho} + 2\rho + \frac{\dot{G}}{G}\rho\frac{a}{\dot{a}}\right). \tag{21}$$

Equation (21) differs from the accustomed equation by accounting for the time derivative of G.

The time derivative of the density $\dot{\rho}$ contains the pressure P responsible for the expansion. The 1. Law of Thermodynamics states that $\mathrm{d}W + P\mathrm{d}V = 0$. We have

$$\frac{\mathrm{d}W}{\mathrm{d}t} + P\frac{\mathrm{d}V}{\mathrm{d}t} = 0. \tag{22}$$

The rate of volume change is

$$\frac{\mathrm{d}V}{\mathrm{d}t} = \frac{32\pi}{3}\frac{\mathrm{d}}{\mathrm{d}t}\left(r^3\right) = 3V\frac{\dot{a}}{a}. \tag{23}$$

On the other hand the change of work is

$$\frac{\mathrm{d}W}{\mathrm{d}t} = V\dot{\rho}c^2 + \rho c^2 \frac{\mathrm{d}V}{\mathrm{d}t} = Vc^2\left(\dot{\rho} + 3\rho\frac{\dot{a}}{a}\right). \tag{24}$$

Now, by combining Equations (23) and (24) with Equation (22) we have

$$\dot{\rho}\frac{a}{\dot{a}} = -3\left(\rho + \frac{P}{c^2}\right). \tag{25}$$

We may now write the complete equation of acceleration

$$\frac{\ddot{a}}{a} = -\frac{4\pi G}{3}\left[\rho\left(1 - \frac{\dot{G}}{G}\frac{a}{\dot{a}}\right) + 3\frac{P}{c^2}\right]. \tag{26}$$

It is easy to show that $\frac{\dot{G}}{G}\frac{a}{\dot{a}} = -1$. When G, ρ_{mx} and P_E from Equations (15), (16) and (17) are substituted into Equation (26), the result is 0. This can be interpreted as the equation being correct, as well as the variable definitions, and that the need for the cosmological constant is necessary. However, we have solved the problem in a more plausible way, the difference between the density and the pressure (divided by c^2) terms must be diminutive. Therefore we introduce a factor $B + 1$ before the pressure term. B is small, roughly $1/\pi^2$, a more precise definition will be presented in Section 4.4. The new acceleration equation is

$$\frac{\ddot{a}}{a} = \frac{c^2}{2r^2}B. \tag{27}$$

We use the following relation as an Ansatz:

$$g = r_0\ddot{a} = \frac{Bc^2}{2r_0 a} = \frac{Bc^2}{2r}. \tag{28}$$

Here g has been used as the symbol for acceleration because a is reserved for the scale factor.

We conclude that r^2 in the denominator of Equation (27) should be multiplied with π^2 (cf. **Figure 2**) to indicate that $\ddot{a}$ is an intrinsic 3d acceleration acting at each point of the space and giving rise to a Coriolis effect.

4.2. The Hubble Parameter

By integrating Equation (27) we obtain the rate of the universe expansion, *i.e.* the Hubble parameter. First

$$\dot{a}\mathrm{d}\dot{a} = \frac{c^2}{r_0^2}B\frac{\mathrm{d}a}{a}, \tag{29}$$

and further

$$\dot{a} = \frac{c}{r_0}\sqrt{B\ln\frac{a}{a_i}} = \frac{c}{r_0}\sqrt{B\ln\frac{r}{r_i}}. \tag{30}$$

This is the Hubble parameter, $a_i = r_i/r_0$. As a first approximation we use $B = 1/\pi^2$ and obtain

$$h_0 = \frac{c}{\pi r_0}\sqrt{\ln\frac{r_0}{r_i}} = 2.229\times10^{-18}\ \mathrm{s}^{-1} \sim H_0 = 68.8\frac{\mathrm{km}}{\mathrm{s}\cdot\mathrm{Mpc}}. \tag{31}$$

H_0 is close to the present best value of 67.7 km/sMpc.

4.3. The Age of the Universe

The passage of time since the initial event is thought to be anchored to the curvature radius due to the relation $\ell_p/t_p = c$, where ℓ_p and t_P are the Planck length and the Planck time respectively, that is, length and time are synchronized even if the pull of gravity changes. Accordingly, we can treat universe size and time as synchronized variables, without considering the decreasing G.

The propagation of time is obtained by integration. We substitute $u = \ln(a/a_i)$ into Equation (30)

$$\int a_i \frac{e^u du}{\sqrt{u}} = \int \frac{c}{r_0}\sqrt{B}dt. \tag{32}$$

The integral on the left-hand side has an error function solution

$$\int a_i \frac{e^u du}{\sqrt{u}} = -a_i i\sqrt{\pi} \cdot erfi\left(\sqrt{u}\right). \tag{33}$$

The real part solution of the right-hand side is obtained by using the Dawson integral function $D_+\left(\sqrt{\ln(a/a_i)}\right)$, to be found in Wolfram-Alpha.

The time as a function of the radius is obtained from

$$t(r) = D_+\frac{2r}{c\sqrt{B}}. \tag{34}$$

In our first approximation $D_+\left(\sqrt{\ln(r_0/r_i)}\right) = 0.05111$, $B = 1/\pi^2$ we get the age of the universe: $t_0 = 4.51 \times 10^{17}$ s ~ 14.3 Gyr, a slightly higher value than the official 13.8 Gyr.

4.4. A Specified Estimate of the Hubble Parameter and Universe Age

Our attempt is to determine B as a function of time. It can be proved that $\lim\left(\sqrt{L}D_+\left(\sqrt{L}\right)\right) = 1/2$ for $\sqrt{L} \to \infty$. We define a parameter

$$v_B = \frac{1}{4LD_+^2}, \tag{35}$$

where $L = \ln(r/r_i) + 1/4$. The addition of 1/4 stems from the need of considering the momentum change caused by the continuous influx of new matter. The momentum force is

$$\begin{aligned} F_M &= \frac{dp}{dt} = M_u\frac{\partial V_u}{\partial t} + V_u\frac{\partial M_u}{\partial t} = M_u\frac{\partial V_u}{\partial r}\frac{dr}{dt} + V_u\frac{\partial M_u}{\partial r}\frac{dr}{dt} \\ &= 8\pi brB\left(\ln\frac{r}{r_i} + \frac{1}{4}\right) = 8\pi brBL, \end{aligned} \tag{36}$$

where $p = M_u V_u$ is the momentum and V_u the velocity of expansion.

It can be shown that

$$B = \left(\frac{v_B}{\pi}\right)^2. \tag{37}$$

As r goes towards ∞, v_B approaches 1 and $B \to 1/\pi^2$. The universe is becoming flat and the frontier speed, see next section, is asymptotically approaching the speed of light.

Substituting L = 96.656 and D_+ = 0.0511248 into Equation (35) results in v_B = 0.98957, which in turn substituted into Equation (37) results in B = 0.099219.

The new Hubble parameter estimate is $h_0 = 2.2075 \times 10^{-18}$ 1/s ~ H_0 = 68.12 km/(s·Mpc).

The corrected universe age is $t_0 = 4.56 \times 10^{17}$ s = 14.46 Gyr.

4.5. Proper Distance and Light Cone Diagram

The cosmic age to proper distance (light cone) diagram is a central tool in judging the actual observable universe relative to the theoretical one. Because the expansion frontier is progressing at almost the speed of light, even near parts of our neighbourhood are disappearing.

We presume that the radius of the frontier of the expanding universe is $r_F = r/\pi$. From Equation (31) the velocity of the frontier expansion is

$$V_F = \frac{c}{\pi}\sqrt{B\ln\left(\frac{r}{r_i}\right)} = vc, \tag{38}$$

where the relative velocity is $v = V_F/c \le 1$.

The calculation of the proper distance requires the geometric representation in Figure 3. Our task is to determine the radius x as a function of the cosmic age t_x. The perimeter of a circle of x represents the proper distance d_p at $t = t_x$.

We define a time factor

$$k_x = \frac{2\pi D_+}{\sqrt{B}}, \tag{39}$$

such that $t_x = k_x r_F/c$, $t_0 = k_{0^*} r_{F0}/c$ and D_+ = Dawson integral function.

From Figure 3 we deduce

$$c^2\left(t_0 - t_x\right)^2 = r_{F0}^2 + r_F^2 - 2r_{F0}\sqrt{r_F^2 - x^2}, \tag{40}$$

where from x is solved. Let $\kappa = x/r_{F0}$ be the normalized radius of x. From Equation (40) we then have

$$\kappa^2 = a^2 - \left[\frac{1}{2}\left(1-k_{x0}^2\right) + \frac{a^2}{2}\left(1-k_x^2\right) + k_x k_{x0} a\right]^2. \tag{41}$$

The proper distance is obtained from

$$d_p = 2\kappa r_0. \tag{42}$$

The relation between the cosmic age and the proper distance is shown in Figure 4. The computed curve (green) according to Equation (42) is compared to results originally published by T. H. Davis and C. H. Lineweaver, [18], however updated with Planck 2013 satellite data, as published by N. Crichton in 2015, [19]. The shapes of the curves are almost identical, though the calculated curve shows a 5% higher maximum value.

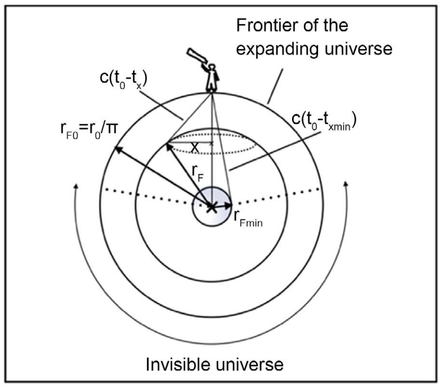

Figure 3. Geometry for the determination of the proper distance.

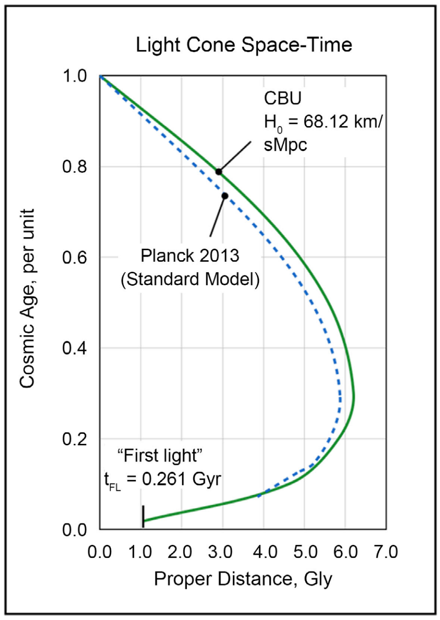

Figure 4. The light cone diagram showing the cosmic age as a function of the proper distance.

In **Figure 5**, the projection of the universe is shown as the surface of a cone with logarithmic scaling. The radius of the observable universe is the half-perimeter of the end circle. The real observable universe is just a small part of the surface, the fast expansion prevents light from the neighbouring areas to reach the observer. In **Figure 6**, the time scale is linear, the radial scale logarithmic. The projection reaches from the time of the CMB to the present. Usually, the universe is described with similar images.

4.6. Coriolis Effect on Celestial Dynamics

It was argued in Section 4.1 that the acceleration is an intrinsic 3d phenomenon that operates at any point in the universe. In rotating systems of fluids, particle clouds or star clusters, acceleration causes a Coriolis effect with a large impact on the dynamical patterns. This is best demonstrated by satellite images of low-pressure rotation on weather maps, or of hurricanes or typhoons, Figure 7.

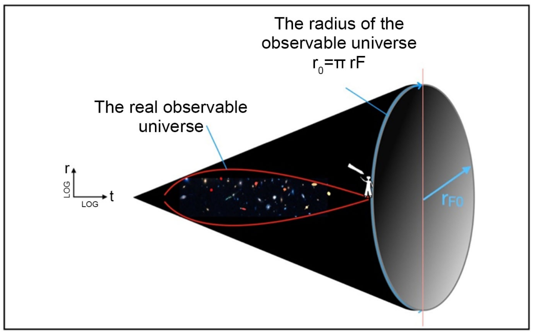

Figure 5. The 2d universe on the time-cone surface. The observable segment represents the curve of Figure 4. Due to the fast expansion light from outside the segment cannot reach an observer on the Earth.

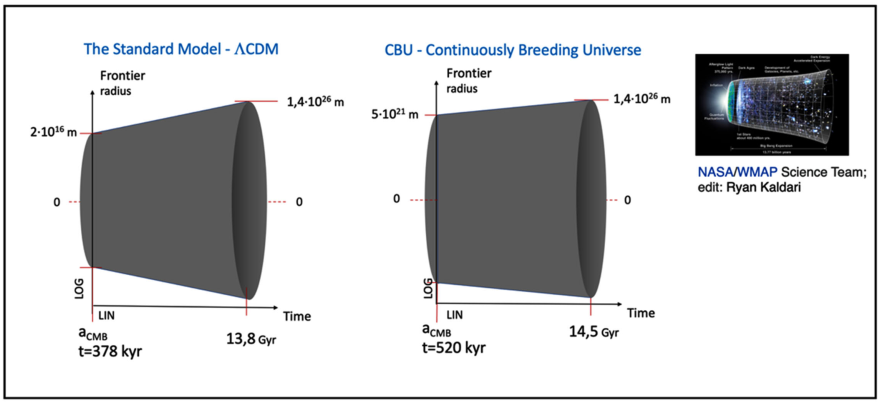

Figure 6. Comparison of the 2d projections of the standard and the CBU model along a linear time axis. The data of the CBU a_{CMB} is calculated in Chapter 7. The NASA image to the upper right is aesthetically attractive but misleading, the star sky should be a projection on the 2d surface of the cone-shaped figure.

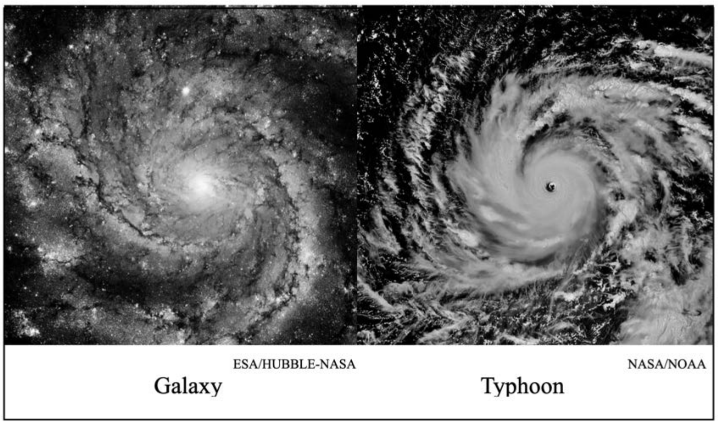

Figure 7. A comparison showing the similarity between the rotation images of a galaxy and a typhoon. It is a known fact that the spiral pattern of the latter is caused by the Coriolis effect.

Here we present a short analysis of the mathematical background of the Coriolis effect. In Figure 8 an observer is located at point O. The observer is studying the velocity relative to coordinate system A of an object at point P. The position vectors are defined as follows

$$\boldsymbol{X}_A = \sum_1^3 x_i \boldsymbol{e}_i, \tag{43}$$

and

$$\boldsymbol{X}_O = \boldsymbol{X}_{OA} + \boldsymbol{X}_A, \tag{44}$$

where $\boldsymbol{e}_i$ is the unit vector.

The observer measures the velocity

$$\frac{\mathrm{d}\boldsymbol{X}_O}{\mathrm{d}t} = \boldsymbol{V}_{OA} + \boldsymbol{V}_A + \sum_1^3 x_i \frac{\mathrm{d}\boldsymbol{e}_i}{\mathrm{d}t} = \frac{\mathrm{d}\boldsymbol{X}_{OA}}{\mathrm{d}t} + \sum_1^3 \frac{\mathrm{d}x_i}{\mathrm{d}t}\boldsymbol{e}_i + \sum_1^3 x_i \frac{\mathrm{d}\boldsymbol{e}_i}{\mathrm{d}t}, \tag{45}$$

where $\boldsymbol{V}_{OA}$ is the velocity difference between the systems, $\boldsymbol{V}_A$ is the velocity of P in A. The last term is the rate of expansion. The observer measures an acceleration g_{obs} of P according to

$$\boldsymbol{g}_{obs} = \frac{\mathrm{d}^2\boldsymbol{X}_O}{\mathrm{d}t^2} = \boldsymbol{g}_{OA} + \frac{\mathrm{d}\boldsymbol{V}_A}{\mathrm{d}t} + \sum_1^3 \frac{\mathrm{d}x_i}{\mathrm{d}t}\frac{\mathrm{d}\boldsymbol{e}_i}{\mathrm{d}t} + \sum_1^3 x_i \frac{\mathrm{d}^2\boldsymbol{e}_i}{\mathrm{d}t^2}. \tag{46}$$

The time derivative $\mathrm{d}\boldsymbol{V}_A/\mathrm{d}t$ represents the "true" (in the reference frame of A) acceleration of the body at P. By derivation of the middle term in Equation (45) we obtain

$$\boldsymbol{g}_{tru} = \frac{\mathrm{d}\boldsymbol{V}_A}{\mathrm{d}t} = \sum_1^3 \frac{\mathrm{d}x_i^2}{\mathrm{d}t^2}\boldsymbol{e}_i + \sum_1^3 \frac{\mathrm{d}x_i}{\mathrm{d}t}\frac{\mathrm{d}\boldsymbol{e}_i}{\mathrm{d}t}. \tag{47}$$

The first term in the latter part represents the Newtonian acceleration g_N. The second term is the result of expansion.

Most galaxy systems are disk-like, therefore we assume the system A being a 2-dimensional cylindrical coordinate system with x_3 coordinates set to 0. The equations of the transformation between the Cartesian and the cylindrical system are

$$x_1 = r_l \cos\theta, \tag{48}$$

$$x_2 = r_l \sin\theta, \tag{49}$$

and

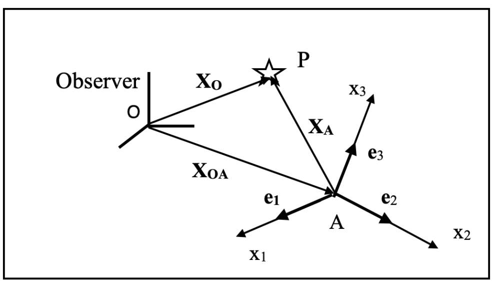

Figure 8. An observer in system O measures the velocity of an object at P in system A, [6].

$$\boldsymbol{e}_x = \cos\theta \boldsymbol{e}_r - \sin\theta \boldsymbol{e}_\theta, \tag{50}$$

$$\boldsymbol{e}_y = \sin\theta \boldsymbol{e}_r + \cos\theta \boldsymbol{e}_\theta, \tag{51}$$

Here r_l is the radial coordinate of the system A.

Next we substitute variables and unit vectors into Equations (46) and (47), and obtain

$$\begin{aligned} \boldsymbol{g}_{obs} = \frac{\mathrm{d}\boldsymbol{V}_{OA}}{\mathrm{d}t} = \boldsymbol{g}_{OA} + \boldsymbol{g}_{tru} + \left(r_l \frac{\mathrm{d}^2 e_r}{\mathrm{d}t^2} + \frac{\mathrm{d}r_l}{\mathrm{d}t}\frac{\mathrm{d}e_r}{\mathrm{d}t} \right)\boldsymbol{e}_r \\ - \left(\frac{\mathrm{d}\theta}{\mathrm{d}t}\frac{\mathrm{d}r_l}{\mathrm{d}t} + r_l \frac{\mathrm{d}^2\theta}{\mathrm{d}t^2} + r_l \frac{\mathrm{d}\theta}{\mathrm{d}t}\frac{\mathrm{d}e_\theta}{\mathrm{d}t} \right)\boldsymbol{e}_\theta, \end{aligned} \tag{52}$$

and

$$\boldsymbol{g}_{tru} = \frac{\mathrm{d}\boldsymbol{V}_A}{\mathrm{d}t} = \left(\frac{\mathrm{d}^2 r_l}{\mathrm{d}t^2} + \frac{\mathrm{d}r_l}{\mathrm{d}t}\frac{\mathrm{d}e_r}{\mathrm{d}t} \right)\boldsymbol{e}_r + \left(\frac{\mathrm{d}\theta}{\mathrm{d}t}\frac{\mathrm{d}r_l}{\mathrm{d}t} + r_l \frac{\mathrm{d}^2\theta}{\mathrm{d}t^2} + r_l \frac{\mathrm{d}\theta}{\mathrm{d}t}\frac{\mathrm{d}e_\theta}{\mathrm{d}t} \right)\boldsymbol{e}_\theta. \tag{53}$$

As the tangential centripetal velocities are of special interest, we concentrate on the radial acceleration components $\boldsymbol{g}_{obs}$ and $\boldsymbol{g}_{tru}$. We denote:

$g_N = \mathrm{d}^2 r_l / \mathrm{d}t^2$, Newtonian gravitational acceleration in radial direction,

$g_{exp} = r_l \left(\mathrm{d}^2 e_r / \mathrm{d}t^2 \right)$, intrinsic expansion acceleration,

$\mathrm{d}r_l / \mathrm{d}t = V_{r_l} = \sqrt{g_N / r_l}$,

$\mathrm{d}e_r / \mathrm{d}t = V_{exp} / r_l = \sqrt{g_{exp} / r_l}$ = increase of local space.

We then define

$$g_{kic} = \frac{\mathrm{d}r_l}{\mathrm{d}t} \cdot \frac{\mathrm{d}e_r}{\mathrm{d}t} = \frac{V_{rl} V_{exp}}{r_l} = \sqrt{g_N g_{exp}}. \tag{54}$$

The equations of the local radial accelerations are

$$g_{tru} = g_N + g_{kic} = g_N + \sqrt{g_N g_{exp}}, \tag{55}$$

$$g_{obs} = g_{tru} + g_{kic} + g_{exp}. \tag{56}$$

The velocity of an object orbiting in A obeys the law of centripetal force

$$V_{orbit} = \sqrt{r_l g}, \tag{57}$$

where g is either g_{obs} or g_{tru}.

Figure 9 shows true and observed accelerations from different published sources. The observation curves are compared with calculated functions based on Equations (55) and (56).

Results published by McGaugh *et al.*, [20] [21], indicate that for decreasing g_N the acceleration declines asymptotically towards $\hat{g}$ = 0.92 × 10^{-11} m/s^2. The number is close to the intrinsic acceleration $g_{exp} = g_0$ = 1.0533 × 10^{-11} m/s^2 from Equation (28).

The MOND theory was developed by M. Milgrom early in the 1980ies, [22]. The MOND curve in Figure 9 follows almost exactly the theoretical Coriolis solution: $g_{MOND} \approx g_N + 2g_{kic}$, without the additional g_{exp} term of Equation (56).

The comparison convincingly confirms that the Coriolis approach provides a credible explanation to the dynamic behavior of the galaxies.

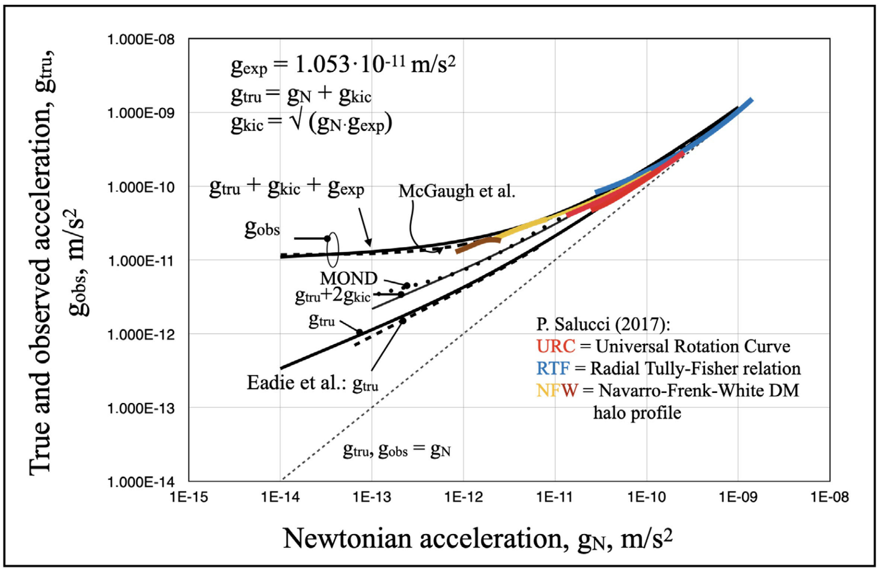

Figure 9. Observed and true acceleration versus the Newtonian acceleration. The full lines are calculated according to the CBU theory. Dashed curves show 1) the observed statistical results of McGaugh *et al.*, [20] [21], and 2) the reconstruction of the Eadie *et al.* Bayesian mass estimates of the Milky Way, [23]. The dotted curve is a calculated version of the MOND acceleration. Colored curves are based on the figure published by Paolo Salucci, [24].

In [6] the rotational velocities of the Milky Way were calculated according to the equations presented here. A spherical bulge and a thin disk, total masses $m_{MW} = 2.3 \times 10^{41}$ kg and $m_{bulge} = 0.29 \times 10^{41}$ kg, were used as a model of the galaxy. The acceleration as a function of the radius r_{MW} was obtained from gravitational potential computations. **Figure 10** shows that the calculated V_{obs} ($= \sqrt{r_l g_{obs}}$) curve follows almost perfectly an average path of Lamost measurements, [25].

5. Quantum Creation

This chapter shows how a solution to the Schrödinger equation at the initial event leads to the introduction of time-dependent Planck units, the influx of new matter and the expansion of space. The energy of the new matter is balanced by the distance extension and thus the increase in the negative gravitational potential energy.

5.1. The Schrödinger Equation

The time-dependent Schrödinger equation is

$$\nabla^2\psi + \frac{8\pi^2 m_e}{h^2}\left(E_i - U_i\right)\psi = 0, \tag{58}$$

where ψ is the quantum-mechanical wave function, E_i is the ground state energy, $U_i = 4\pi b r_i^2$ is the potential energy. The spherically symmetric form of Equation (58) is

$$\frac{\partial^2\psi}{\partial r^2} + \frac{2}{r}\frac{\partial\psi}{\partial r} + \frac{8\pi^2 m_e}{h^2}E_i\psi - \frac{32\pi^3 m_e b}{h^2}r^2\psi = 0, \tag{59}$$

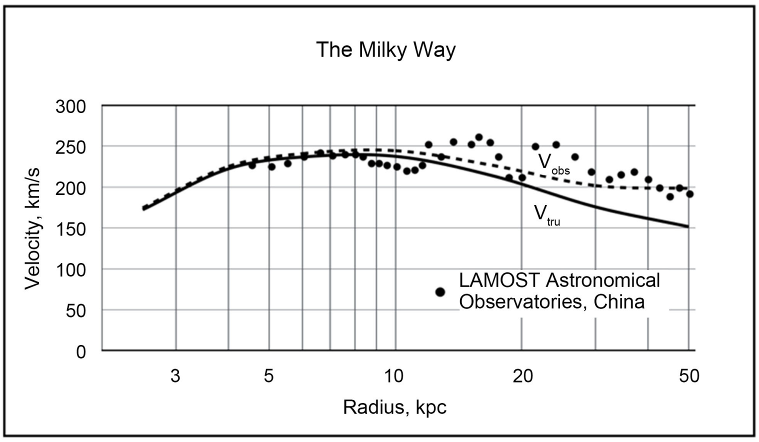

Figure 10. The rotational velocity distribution of the Milky Way. The curves are calculated according to the CBU theory, the points are from Lamost [25]. The figure from [6].

where r is the curvature radius and b the energy constant of Equation (14).

Let

$$\frac{a_1^4}{4} = \frac{h^2}{32\pi^3 m_e b}, \tag{60}$$

$$C = \frac{8\pi^2 m_e}{h^2} E_i. \tag{61}$$

The Schrödinger equation takes the form

$$\frac{\partial^2 \psi}{\partial r^2} + \frac{2}{r}\frac{\partial \psi}{\partial r} + C\psi - \frac{4}{a_1^4} r^2 \psi = 0. \tag{62}$$

This Sturm-Liouville type differential equation has the solution

$$\psi(r) = \frac{1}{r} \mathrm{e}^{-\left(\frac{r}{a_1}\right)^2} \left\{ c_1 H_n\left(\frac{r}{a_1}\right) + c_2 \left|F\right|_{(a;b;x)} \left[\frac{1}{4}\left(1 - Ca_1^2\right); \frac{1}{2}; \left(\frac{r}{a_1}\right)^2\right]\right\}, \tag{63}$$

where H_n is the Hermite polynomial function and $\left|F\right|_{(a;b;x)}$ is the Kummer confluent hypergeometric function. c_1 and c_2 are constants of integration.

The constant a_1 is in a key position

$$a_1 = \sqrt{\frac{h}{2\pi} \frac{1}{\sqrt{2\pi b m_e}}}. \tag{64}$$

By substituting b from Equation (14) we have

$$\frac{1}{\sqrt{2\pi b m_e}} = \frac{r_i}{m_e c}, \tag{65}$$

and by substituting G_i from Equation (7) we have

$$a_1 = \sqrt{\frac{hG_i}{2\pi c^3}} = \ell_{Pi}. \tag{66}$$

By definition ℓ_{Pi} is the Planck length of the virgin universe. In the CBU theory the Planck length is dependent on the radius r and time. The numerical value is $\ell_{Pi} = 1.43516 \times 10^{-14}$ m.

It can be shown that

$$\left(\frac{\ell_{Pi}}{2r_i}\right)^2 = \frac{2\pi - 1}{4\alpha_{fs}}, \tag{67}$$

where α_{fs} is the fine structure constant, 1/137.036. The result is not a coincidence, but a purely physical relation based on known physical constants. The equation emphasizes the significance of the Planck scale and the curvature radius r_i of the virgin universe. It might be seen as a proof of the connection between gravity and quantum mechanics.

Equation (67) *reflects the intuitive thought expressed by Richard Feynman in the* 1950*ies*: "137 *holds the answers to the Universe*", [26].

Here is the confirmation.

Substituting G from Equation (15) into Equation (66) we obtain a general expression for the Planck length

$$\ell_P(r) = \ell_{Pr} = \frac{1}{2\pi}\sqrt{\frac{hc}{br}}. \tag{68}$$

A simple check using $r_0 = 4.20550 \times 10^{26}$ m shows that the Planck length according to Equation (68) results in 1.61625×10^{-35} m, which exactly equals the current official value.

In analogy with the hydrogen atom the ground state energy E_{GSi} is postulated to be of the form

$$E_{GSi} = \frac{h^2}{8m_e\ell_{Pi}^2} = \frac{hc}{4\pi r_i}. \tag{69}$$

The general expression of the instantaneous ground state energy takes the form

$$E_{GS}(r) = E_{GSr} = \frac{h^2}{8m_e\ell_{Pi}\ell_{Pr}} = \frac{\pi hc\ell_{Pi}}{4\ell_{Pr}r_i} = \pi^2\frac{\ell_{Pi}}{2r_i}\sqrt{hcbr}. \tag{70}$$

The Planck energy W_P has an important bearing on the influx of new matter. By definition

$$W_{Pi} = \sqrt{\frac{hc^5}{2\pi G_i}} = \frac{\ell_{Pi}}{r_i}W_e. \tag{71}$$

At the initial event a positron and an electron are exited, from Equation (71) we deduce that the particles originate from

$$2W_e = \frac{W_{Pi}}{\ell_{Pi}/2r_i}. \tag{72}$$

The significance of $\ell_{Pi}/2r_i = 13.453499$ in the CBU theory is obvious here, if W_{Pi} is considered the virtual dark energy of the virgin universe, then the real energy is obtained by dividing it with the ratio $\ell_{Pi}/2r_i$.

The general expression for $W_P(r) = W_{Pr}$ is

$$W_{Pr} = \sqrt{hcbr}. \tag{73}$$

For $r = r_0$, W_{Pr} is 1.9560815 × 10^9 J, which is in full compliance with the official value.

A comparison of Equation (73) with Equation (70) shows the relation between the Planck and ground state energy

$$E_{GSr} = \pi^2 \frac{\ell_{Pi}}{2r_i} W_{Pr}. \tag{74}$$

5.2. Generalized Uncertainty

The temporal change of the gravity strength and the momentum has an impact on the uncertainty window, *i.e.* $\Delta p \Delta x$, which constitutes the classical Heisenberg formulation, cf. Ronald D. Adler [27]. We divide Δx into a Heisenberg component $\Delta x_H = h/(4\pi \Delta p_H)$ and a gravity component

$$\Delta x_g = \frac{h}{4\pi \Delta p_g}. \tag{75}$$

The momentum uncertainty is

$$\Delta p = \frac{\mathrm{d}p}{\mathrm{d}r} \ell_{Pr}. \tag{76}$$

We have

$$\frac{\mathrm{d}p}{\mathrm{d}r} = \frac{8\pi br}{c} \sqrt{BL} \left(1 + \frac{1}{4L}\right), \tag{77}$$

where the term containing $1/4L$ is due to the fact that L is a $\ln(r)$ function.

Presuming that the location uncertainty is $\Delta x = \ell_{Pr}/2$, we have

$$\Delta p \Delta x_H \le \frac{1}{2} \frac{\mathrm{d}p}{\mathrm{d}r} \ell_{Pr}^2 = \frac{h}{4\pi} f_r, \tag{78}$$

where $\Delta p = f_r \cdot \Delta p_H$ and

$$f_r = 4\sqrt{BL} \left(1 + \frac{1}{4L}\right). \tag{79}$$

Adler has derived an expression for the gravity component

$$\Delta x_g = \pi \frac{\Delta p \ell_{Pr}^2}{h} = \frac{h}{4\pi \Delta p} \left(\frac{2\pi \ell_{Pr} \Delta p}{h}\right)^2. \tag{80}$$

After some algebraic manipulation we arrive at the final uncertainty equation

$$\Delta p \Delta x = \Delta p \left(\Delta x_H + \Delta x_g\right) \le \frac{h}{4\pi} \left(f_r + f_r^2\right) = \frac{h}{4\pi} F_r, \tag{81}$$

where $F_r = f_r(1 + f_r)$ is the overall uncertainty factor and $\Delta p = F_r \cdot \Delta p_g$. When f_r is substituted into F_r, we obtain a proximity value to the real uncertainty factor: $F_{rU} = 4\sqrt{BL} \cdot (\ell_{Pi}/2r_i)$, which applies to the *universe BH*. A similar analysis leads to $F_{rB} = \sqrt{BL} \cdot (\ell_{Pi}/2r_i)$ for the *galaxy BH*.

We verify the validity of F_{rU} by substituting Equation (79) into $F_r = f_r(1 + f_r)$, we have

$$\frac{F_{rU}}{4\sqrt{BL}} = (1+1/4L)\left[1+4\sqrt{BL}(1+1/4L)\right] = 13.4539. \tag{82}$$

The result shows the resemblance with $\ell_{Pi}/2r_i = 13.4535$. It also proves that the reasoning of R.D. Adler is correct. We should consider the mathematical model as an approximation of the quantum process behind the injection of real matter particles.

A detailed analysis of the physics of *galaxy BH*s will be presented in Chapter 8.

5.3. Matter Influx

5.3.1. Universe Inside

The leading paradigm of the CBU theory says that we live inside a low-density black hole and that the expansion is explained by a continuous "creation" of matter. As our main postulate we assume that the matter influx originates from virtual dark energy. The dark energy is a state of the quantum or QED vacuum, which due to the uncertainty principle allows particles to enter the real-world space (inside the universe BH) and simultaneously increase the space. The influx rate is obtained from the virtual dark energy, W_{vDE}, time change

$$\frac{\mathrm{d}W_{vDE}}{\mathrm{d}t} = \frac{W_{Pr}}{t_P}F_{rU} = \frac{cW_{Pr}}{\ell_{Pr}}F_{rU}, \tag{83}$$

where $t_P = \ell_{Pr}/c$ is the Planck time. When the functions of W_{Pr}, ℓ_{Pr} and F_{rU} are substituted into Equation (83) we have

$$\frac{\mathrm{d}W_{vDE}}{\mathrm{d}t} = 8\pi brc\sqrt{BL}\cdot\frac{\ell_{Pi}}{2r_i}. \tag{84}$$

On the other hand, we have an increase of real matter (and radiation) according to

$$\frac{\mathrm{d}W_u}{\mathrm{d}t} = \frac{\mathrm{d}W_u}{\mathrm{d}r}\cdot\frac{\mathrm{d}r}{\mathrm{d}t} = 8\pi brc\sqrt{BL}, \tag{85}$$

meaning that

$$\frac{W_{vDE}}{W_u} = \frac{\ell_{Pi}}{2r_i} = \frac{\Omega_\Lambda}{\Omega_b}, \tag{86}$$

where Ω_Λ is the normalized dark energy density and Ω_b is the normalized baryon density, in practice the normalized real energy density. For a typical $\Omega_\Lambda = 0.68$ we have $\Omega_b = 0.050$ (officially 0.049).

Equation (86) *is an important result, because it provides a constant ratio value between the virtual dark energy density and the real energy density. The ratio is confirmed by observations. The equation also proves that the assumptions leading to the definition of the generalized uncertainty factor F_{rU} are most likely.*

There is also another route to establish Equation (86). The pressure responsible for the expansion can be linked to the energy density of the virtual dark energy as follows

$$-\frac{P_{EM}}{c^2} = -\frac{P_E}{c^2} - \frac{P_M}{c^2} = \frac{b}{4c^2r}(1+2BL) = \frac{2}{3}\rho_{mx}(1+2BL) = \rho_{vDE}. \tag{87}$$

Here the Eulerian pressure P_E is obtained from Equation (17) and the momentum pressure is derived using the momentum force from Equation (36)

$$P_M = \frac{F_M}{A_u} = -\frac{b}{2r} BL. \tag{88}$$

From Equation (86) we have

$$\frac{W_{vDE}}{W_u} = \frac{\rho_{vDE}}{\rho_{mx}} = \frac{\ell_{Pi}}{2r_i} = \frac{2}{3}(1+2BL). \tag{89}$$

When the physical expression of $\ell_{Pi}/2r_i$ of Equation (67) is substituted into Equation (89), we obtain an exact equation for the current value of BL

$$B_0 L_0 = \frac{1}{2}\left(\frac{3}{2}\sqrt{\frac{2\pi-1}{4\alpha_{fs}}} - 1\right) = 9.590125. \tag{90}$$

5.3.2. The Quantum Vacuum Energy

The ground state energy of the initial event as obtained from Equation (70) is

$$E_{GSi} = \pi^2 \frac{\ell_{Pi}}{2r_i} W_{Pi} = 2\pi^2 \left(\frac{\ell_{Pi}}{2r_i}\right)^2 \cdot W_e, \tag{91}$$

where W_e is the rest energy of the electron.

It appears that $\pi^2 \cdot \left(\frac{\ell_{Pi}}{2r_i}\right)^2 = \pi^2 \cdot (2\pi - 1)/4\alpha_{fs} = 1786$ *is very close to the ratio* $W_p/W_e = 1836.15$. *This is probably not a coincidence. The electron and the proton are the most stable particles of the universe, it seems quite logical that the universe started with the emergence of a proton-antiproton pair at the outer Schwarzschild boundary and a positron-electron pair on the inner photon sphere.* We postulate that there is a B factor ν_{Bi} such that

$$\frac{W_p}{W_e} = \frac{\pi^2}{\nu_{Bi}^2}\left(\frac{2\pi-1}{4\alpha_{fs}}\right) = \frac{1}{B_i}\left(\frac{2\pi-1}{4\alpha_{fs}}\right). \tag{92}$$

For $\nu_{Bi} = 0.9863493$ we have $B_i = 0.0985739$. The result of Equation (92) is 1836.15. As we see, B varies within very small limits, $B = 0.098574 - 0.099219$ between "creation" and the present.

Next, our goal is to determine the level of the current ground state energy E_{GS0}. From Equation (70) we have that $E_{GS} = \text{constant} \cdot \sqrt{r}$. The number of electron-positron pairs is

$$N_{e^+e^-} = \left(\frac{r}{r_i}\right)^2. \tag{93}$$

The same equation is valid for the Dirac's Large Number Hypothesis (LNH). Similarly, we can calculate the number of protons and antiprotons exited on the Schwarzschild boundary

$$E_{GSr} = 2\nu_{Bi}^2 W_P \sqrt{\frac{r}{r_i}}. \tag{94}$$

In the current state of the universe E_{GS0} equals 2.597×10^{11} J, a very small number. It is not clear where these protons and antiprotons are located, but an interpretation of the ground state from the electron-positron side leads to the same equation. *In summary, the proton-antiproton pair forms the virtual quantum vacuum energy for the interior of the black hole.*

The exact value of ν_{Bi} is obtained from the equation

$$\nu_{Bi} = \sqrt{\frac{\pi^2 (2\pi - 1)}{4W_p \nu_{fs}} \cdot \sqrt{hcbr_i}} = 0.9863493. \quad (95)$$

6. General Relativity

6.1. The Einstein Field Equation

The most compact version of the Field Equation is

$$G_{\mu\nu} = 8\pi G T_{\mu\nu}, \quad (96)$$

where $G_{\mu\nu}$ is the Einstein tensor and $T_{\mu\nu}$ is the energy-momentum tensor. Equation (96) has an analytical solution, provided $T_{\mu\nu}$ is isotropic and homogeneous.

One objective of the study is to find a logical solution to the Field Equation without the cosmological constant Λ. We will show that incoming new matter and a variable G affect the energy density and the expansion pressure in a way making Λ unnecessary.

The Einstein tensor is divided into the Ricci curvature tensor $R_{\mu\nu}$ and the Ricci scalar R according to

$$G_{\mu\nu} = R_{\mu\nu} - \frac{1}{2} R g_{\mu\nu}. \quad (97)$$

The components of the $R_{\mu\nu}$ tensor are obtained by using the Christoffel symbols, the procedure is found in any textbook on General Relativity, cf. Carroll [17]. The Ricci tensor is

$$R_{\mu\nu} = \begin{pmatrix} -3\frac{\ddot{a}}{a} & 0 & 0 & 0 \\ 0 & \frac{\ddot{a}}{a} + 2\left(\frac{\dot{a}}{a}\right)^2 + 2k\frac{c^2}{a^2 r_{cur}^2} & 0 & 0 \\ 0 & 0 & \frac{\ddot{a}}{a} + 2\left(\frac{\dot{a}}{a}\right)^2 + 2k\frac{c^2}{a^2 r_{cur}^2} & 0 \\ 0 & 0 & 0 & \frac{\ddot{a}}{a} + 2\left(\frac{\dot{a}}{a}\right)^2 + 2k\frac{c^2}{a^2 r_{cur}^2} \end{pmatrix}, \quad (98)$$

where r_{cur} is the curvature radius and k the curvature parameter according to the Friedmann-Robertson-Walker metrics, k cf. Equation (19).

The Ricci scalar is

$$R = -6\left[\frac{\ddot{a}}{a} + \left(\frac{\dot{a}}{a}\right)^2 + k\frac{c^2}{a^2 r_{cur}^2}\right]. \quad (99)$$

The metric tensor $g_{\mu\nu}$ is

$$g_{\mu\nu} = \begin{pmatrix} 1 & 0 & 0 & 0 \\ 0 & -1 & 0 & 0 \\ 0 & 0 & -1 & 0 \\ 0 & 0 & 0 & -1 \end{pmatrix}. \tag{100}$$

6.2. The Energy-Momentum Tensor

Based on Equations (96) and (99) the unit of the energy-momentum tensor $T_{\mu\nu}$ components are that of a mass density, kg/m^3. The tensor is defined as follows

$$T_{\mu\nu} = \begin{pmatrix} \rho_{eq} & 0 & 0 & 0 \\ 0 & \frac{P_{exp}}{c^2} & 0 & 0 \\ 0 & 0 & \frac{P_{exp}}{c^2} & 0 \\ 0 & 0 & 0 & \frac{P_{exp}}{c^2} \end{pmatrix}. \tag{101}$$

Our task is to find the equivalent density ρ_{eq} and the pressure P_{exp} that accounts for both expansion and acceleration. From Equation (87) we have

$$P_{EM} = -\frac{b}{4r}(1+2BL). \tag{102}$$

The density ρ_{eq} affects the velocity of expansion, *i.e.* the Hubble parameter. It consists of two components

$$\rho_{eq} = \rho_{mx} + \rho_{EM}, \tag{103}$$

where ρ_{EM} is caused by the momentum change, ρ_{mx} is the matter + radiation density.

According to the 1st Law of Thermodynamics we have

$$\frac{dW_{exp}}{dt} + P_{EM}\frac{dV}{dt} = 0, \tag{104}$$

where $W_{exp} = \rho_{EM} c^2 V$, the time derivative of which is

$$\frac{dW_{exp}}{dt} = \dot{\rho}_{EM} c^2 V + \rho_{EM} c^2 \frac{dV}{dt}. \tag{105}$$

Here $dV/dt = 3V\frac{\dot{a}}{a}$. We approximate that

$$\dot{\rho}_{EM} \cong -\rho_{EM}\frac{\dot{a}}{a}. \tag{106}$$

From Equations (104) and (105) we now have

$$\rho_{EM} = -\frac{3}{2}\frac{P_{EM}}{c^2}. \tag{107}$$

Substituting P_{EM} from Equation (102) we have

$$\rho_{EM} = \rho_{mx}(1+2BL), \tag{108}$$

and then Equation (103) becomes

$$\rho_{eq} = \rho_{mx} + \rho_{EM} = 2\rho_{mx}(1+BL). \tag{109}$$

In order to get the total pressure P_{exp} responsible for both expansion and acceleration we need to include the gravitational parameter G into the 1st Law of Thermodynamics

$$\frac{\mathrm{d}\left(GW_{exp}\right)}{\mathrm{d}t}+GP_{exp}\frac{\mathrm{d}V}{\mathrm{d}t}=0, \tag{110}$$

where $W_{exp} = \rho_{eq}c^2 V$. After some manipulations, cf. Section 4.1, we have

$$\frac{\dot{G}}{G}\rho_{eq}+\dot{\rho}_{eq}+3\rho_{eq}\frac{\dot{a}}{a}=-3\frac{P_{exp}}{c^2}\frac{\dot{a}}{a}. \tag{111}$$

From Equation (15) we conclude that $\frac{\dot{G}}{G}=-\frac{\dot{a}}{a}$. Further, we have that $\dot{\rho}_{eq}=2\rho_{mx}\left(B-BL-1\right)\frac{\dot{a}}{a}$. Finally, the pressure is obtained from

$$\frac{P_{exp}}{c^2}=-\frac{2\rho_{mx}}{3}\left(1+B+BL\right). \tag{112}$$

Now the Einstein Field Equation can be completed in a form which eliminates the need for a cosmological constant Λ

$$R_{\mu\nu}-\frac{1}{2}Rg_{\mu\nu}=8\pi GT_{\mu\nu}. \tag{113}$$

6.3. Field Equation Characteristics

All components of the energy-momentum tensor contain $2\rho_{mx}$. By substituting G from Equation (15) and ρ_{mx} from Equation (16) into Equation (113) we arrive at the following expression for the tensor

$$T_{\mu\nu}=3\left(\frac{c}{r_0}\right)^2\begin{pmatrix}\frac{1+BL}{a^2} & 0 & 0 & 0\\ 0 & -\frac{1}{3}\cdot\frac{1+B+BL}{a^2} & 0 & 0\\ 0 & 0 & -\frac{1}{3}\cdot\frac{1+B+BL}{a^2} & 0\\ 0 & 0 & 0 & -\frac{1}{3}\cdot\frac{1+B+BL}{a^2}\end{pmatrix}. \tag{114}$$

where $T_{\mu\nu}$ replaces $8\pi GT_{\mu\nu}$.

Due to substitution G has vanished, the energy-momentum tensor is independent of the gravitational parameter. Making use of the definition of the Hubble parameter in Equation (30) we can write the tensor as follows

$$T_{\mu\nu}=\begin{pmatrix}3\left(h_H^2+\frac{c^2}{a^2r_0^2}\right) & 0 & 0 & 0\\ 0 & -\left(h_H^2+\left(1+B\right)\frac{c^2}{a^2r_0^2}\right) & 0 & 0\\ 0 & 0 & -\left(h_H^2+\left(1+B\right)\frac{c^2}{a^2r_0^2}\right) & 0\\ 0 & 0 & 0 & -\left(h_H^2+\left(1+B\right)\frac{c^2}{a^2r_0^2}\right)\end{pmatrix}. \tag{115}$$

The term $1 + B$ indicates the extra pressure required for acceleration.

The Field Equation written in its most compact form is now

$$G_{\mu\nu} = R_{\mu\nu} - \frac{1}{2} R g_{\mu\nu} = T_{\mu\nu}. \tag{116}$$

The Friedmann-Robertson-Walker temporal equation, which also may be called the *Hubble expansion equation*, is

$$R_{00} - \frac{1}{2} R g_{00} = T_{00}. \tag{117a}$$

We have

$$-3\frac{\ddot{a}}{a} + 3\frac{\ddot{a}}{a} + 3\left(\frac{\dot{a}}{a}\right)^2 + 3k\frac{c^2}{a^2 r_{cur}^2} = 3h_H^2 + 3\frac{c^2}{a^2 r_0^2}. \tag{117b}$$

Further,

$$\left(\frac{\dot{a}}{a}\right)^2 + k\frac{c^2}{a^2 r_{cur}^2} \equiv h_H^2 + \frac{c^2}{a^2 r_0^2}. \tag{117c}$$

By definition $\frac{\dot{a}}{a} = h_H$. $k = 1$ means that the universe is closed. $ar_{cur} = ar_0$ proves that the average curvature radius equals the radius r of the observable universe, a circumstance emphasized by Einstein in the cosmological constant paper [5].

The *acceleration equation* is obtained from

$$R_{ij} - \frac{1}{2} R g_{ij} = T_{ij}, \tag{118}$$

where i and $j = 1, 2, 3$. After some algebraic manipulations and the substitution of Equation (117c) into the equation, we end up with

$$\ddot{a} = \frac{c^2}{2ar_0^2} B \tag{119a}$$

or

$$g = r_0 \ddot{a} = \frac{c^2}{2ar_0} B. \tag{119b}$$

For $a = 1$, $B = 0.099219$ we have $g_0 = 1.0533 \times 10^{-11}$ m/s^2.

The equation corresponds to our Ansatz in Equation (28). The acceleration g is an inherent characteristic of the expanding universe. Over a comoving distance d in the vicinity of an observer, the scale factor a in Equation (119b) equals $1 - d/r_0 \approx 1$ – extremely small influence.

The inherent acceleration g provides a Coriolis effect, which explains the rotational behaviour of the galaxies and the celestial movements at large, and thereby eliminates the need for dark matter, cf. Eriksson [6].

6.4. Energy Conservation

It is important to prove that the $T_{\mu\nu}$ tensor fulfils the temporal energy conservation condition. The general expression using Christoffel symbols Γ is, cf. Carroll [17],

$$\nabla_\mu T^\mu{}_0 = \partial_\mu T^\mu{}_0 + \Gamma^\mu_{\mu 0} T^0{}_0 - \Gamma^\lambda_{\mu 0} T^\mu{}_\lambda = -\partial_0 \rho_{eq} - 3\frac{\dot{a}}{a}\left(\rho_{eq} + \frac{P_{exp}}{c^2}\right) = 0. \quad (120a)$$

The time derivative is

$$\partial_0 \rho_{eq} = \frac{\partial}{\partial t}\left(\frac{1+BL}{a^2}\right) = -\left(\frac{2(1+BL)}{a^2} - \frac{B}{a^2}\right)\left(\frac{\dot{a}}{a}\right). \quad (120b)$$

We have

$$\frac{1}{a^2}(2 + 2BL - B - 3 - 3BL + 1 + B + BL)\left(\frac{\dot{a}}{a}\right) = 0. \quad (120c)$$

The conservation condition is met. The result shows that the components ρ_{eq} and P_{exp}/c^2 are correctly derived.

7. Cosmic Microwave Background Radiation

7.1. Influence of Gravitation on the Redshift

The gravitational parameter G is extremely large in the initial phase, $G_i \approx 5 \times 10^{31}$ m^3/kg/s^2. The parameter decreases successively with the expansion. The photons in the cosmic microwave background (CMB) propagating faster than the expansion start from a deep gravitational well. We write the energy equation of the electromagnetic radiation as a gravitational gradient equation

$$hdf + g\frac{hf}{c^2}dr = 0, \quad (121)$$

where f is the frequency, g the gravitational acceleration along r. We obtain g from

$$g = \frac{GM}{r^2} = \frac{2c^2}{r}. \quad (122)$$

Here we make use of $M = 4\pi br^2/c^2$ and $G = c^4/2\pi br$, cf. Equations (13) and (15). Having that $f = c/\lambda$, $\mathrm{d}f = -c\mathrm{d}\lambda/\lambda^2$ and $r = r_0 a$, where a is the scale factor, we write

$$\int \frac{\mathrm{d}\lambda}{\lambda} = 2\int \frac{\mathrm{d}a}{a}. \quad (123)$$

Integration implies that λ is proportional to a^2. We deduce that

$$\frac{\lambda_0 - \lambda_s}{\lambda_s} = \left(\frac{1-a}{a}\right)^2 = z_g. \quad (124)$$

Here z_g is the gravitational redshift, λ_s and λ_0 are the wavelengths at the source and at the observer respectively.

As known, the cosmological redshift is

$$z_{cr} = \frac{1}{a} - 1. \quad (125)$$

The combined redshift is $z = z_g + z_{cr}$. We have

$$\frac{\lambda_0}{\lambda_s} = \frac{f_s}{f_0} = z + 1 = \frac{1 - a + a^2}{a^2}. \tag{126}$$

Let a_c stand for the scale factor at the CMB event. For vary small values of the scale factor the frequency of CMB photons decrease approximately according to

$$f_0 \approx a_c^2 f_c. \tag{127}$$

John Huchra at the Harvard-Smithsonian Center for Astrophysics has established the addition rule for combining multiple types of redshifts, [28].

An interesting feature of Equation (126) is that the difference between z_{cr} and z changes very slowly for scale factors close to 1. The discrepancies of the current distance estimates in the vicinity of the Milky Way are still within error limits.

Data on proper distances ($d_{p\Lambda}$, d_{pCBU}), lookback times ($t_{\Lambda z}$, $t_{\Lambda}(z_{cr})$ and t_{CBU}) are collected in **Table 1**. Λ refers to the standard ΛCDM model, cf. [29] and [30], and CBU to calculated numbers of the current theory.

In **Figure 11** the data of **Table 1** show the correlation between the ΛCDM and CBU models. There is a good agreement between the lookback time graphs t_{CBU} and $t_{\Lambda z}$. t_{CBU} is based on Equation (34), while $t_{\Lambda z}$ originates from the graph in [29]. z was determined from Equation (126) using the appropriate scale factor. d_{pCMB} was calculated according to a unique algorithm presented in Section 4.5, [6]. Even for the proper distances the similarity between the curves is good considering the different approaches.

The difference between the look-back times $t_{\Lambda}(z_{cr})$ and t_{CBU}, **Figure 12**, is interesting, because it indicates a deviation in the estimates of distant cosmic events. For instance, the most distant observed galaxy Glass-z13 has a redshift of 13, which would mean that a fully developed galaxy had evolved in about 0,35 Gyr after the Big Bang. This is an intriguing paradox; it is most uncertain that billions of stars would have developed in such a short time. According to CBU the lookback time would be 11 Gyr and, considering the age of the universe being 14.4 Gyr, the time for the galaxy to evolve would be a more plausible time of 3.4 Gyr.

Table 1. Lookback time (Gyr) and proper distance (Gly).

Scale factor a	0.1	0.2	0.4	0.6	0.8	0.9
P.u. time, τ_{Λ}	0.05	0.121	0.318	0.556	0.790	0.894
ΛCDM redsh. z_{cr}	6.7	3.71	1.44	0.62	0.24	0.11
Comb.redsh. z	90	20	3.75	1.11	0.313	0.123
Lookback, $t_{\Lambda z}$	13.11	12.6	9.45	6.0	2.90	1.45
Lookback, $t_{\Lambda}(z_{cr})$	13.8	13.5	11.9	8.1	3.43	1.56
Lookback, t_{CBU}	12.9	11.5	8.61	5.74	2.87	1.43
Proper dist. $d_{p\Lambda}$	3.58	4.91	5.82	4.75	2.75	1.42
Proper dist. d_{pCBU}	4.45	5.59	5.74	4.45	2.58	1.31

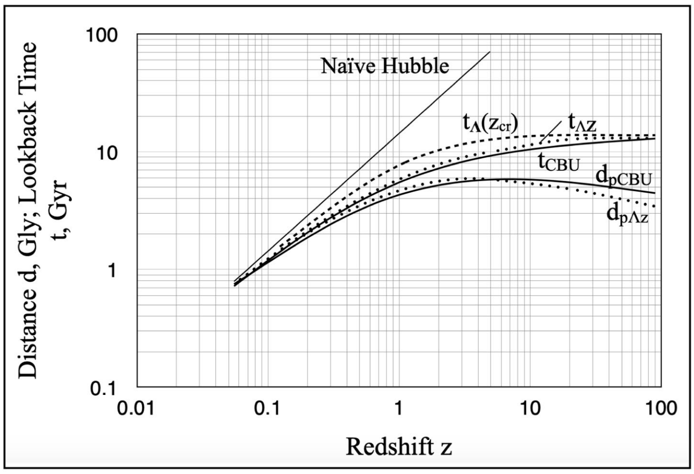

Figure 11. The lookback time and the proper distance as a function of the combined gravitational and cosmological redshift.

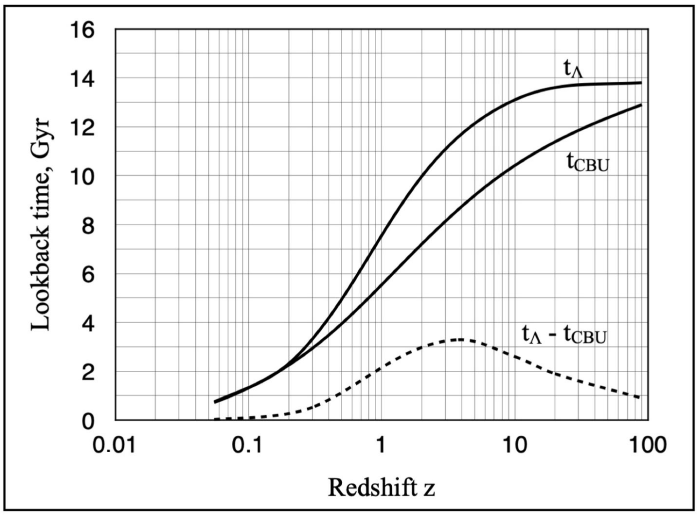

Figure 12. The lookback time as a function of the redshift according to (a) the standard model, $t_\Lambda(z_{cr})$ and (b) to the CBU theory. The deviation is at it's largest, 3.2 Gyr, around $z = 4$.

7.2. The CMB Scale Factor

We obtain the energy density w_{BB} of the black body radiation from the classical Stefani-Boltzmann equation

$$w_{BB} = \frac{8\pi^5 k_B^4}{15c^3h^3}T^4 = \alpha_B T^4. \tag{128}$$

Here $\alpha_B = 4\sigma_{SB}/c = 7.565723 \times 10^{-16}$ J/K^4·m^3 is the radiation density constant, σ_{SB} is the Stefani-Boltzmann constant, and k_B the Boltzmann constant.

The number density of the photons is obtained from, cf. Wikipedia: Photon Gas,

$$n_{ph} = 16\pi\zeta(3)\left(\frac{k_B T}{hc}\right)^3, \tag{129}$$

where $\zeta(3) = 1.202056$ is the Riemann zeta-function. By dividing Equation (128) with Equation (129) we obtain an expression for the photon energy

$$W_{ph} = \frac{\alpha_B T}{16\pi\zeta(3)}\left(\frac{hc}{k_B}\right)^3. \tag{130}$$

If we assume that the photon energy at the CMB event equals one of the two photons caused by the annihilation, we have $W_{phc} = W_e$. The current photon energy is then

$$W_{ph0} = a_c^2 W_e = \frac{\alpha_B T_0}{16\pi\zeta(3)}\left(\frac{hc}{k_B}\right)^3. \tag{131}$$

Accordingly, for $T_0 = 2.72548$ K we have

$$a_{CMB} = a_c = \sqrt{\frac{\alpha_B T_0}{16\pi\zeta(3)}\left(\frac{ch}{k_B}\right)^3 \frac{1}{W_e}} = 3.523\times10^{-5}. \tag{132}$$

Due to the square root the number is much larger than usually suggested (10^{-7} - 10^{-9}).

The current photon energy is $W_{ph0} = 1.0164 \times 10^{-22}$ J and the corresponding frequency $f_0 = W_{ph0}/h = 153.4$ GHz, slightly below the optimum frequency of the Planck black body spectrum of $f_{Imax} = 160.23$ GHz.

7.3. Origin of the CMB

7.3.1. Hypotheses

The primordial universe is the inside of a black hole, where the number of electron-positron pairs increases successively. Some of the electrons and positrons annihilate forming photons. At some point the energy of the photons is equal to the matter energy. We assume that a transition occurs, the photons fill the inner free space of the BH and the matter is concentrated in a multitude of "small" black holes. The photons are entangled in a state of superposition. They do not follow the same rules as photons from an ordinary light source, e.g. a star. We call the transition the CMB event. **Figure 13** shows the universe prior to the transition. After the CMB event, the galaxy black holes initiate an outflow of protons and antiprotons into free space, **Figure 14**.

There are divergent opinions about the destiny of the energy lost by light propagating in the expanding universe. Light waves in a gravitational field are part of the system, gaining or loosing potential energy. The CMB photons, however, are different.

It is a well-known fact that the number density of CMB photons, $n_{ph0} \approx 4 \times 10^8$ ph/m^3, is in poor conformity with a value predicted by e^+ - e^- annihilations, the number requires a boost. The state of superposition offers a novel approach. *The energy lost during the propagation of the light wave is compensated by an addition of the number of photons, which means that photons in a superposition are not a multitude of individual particles.*

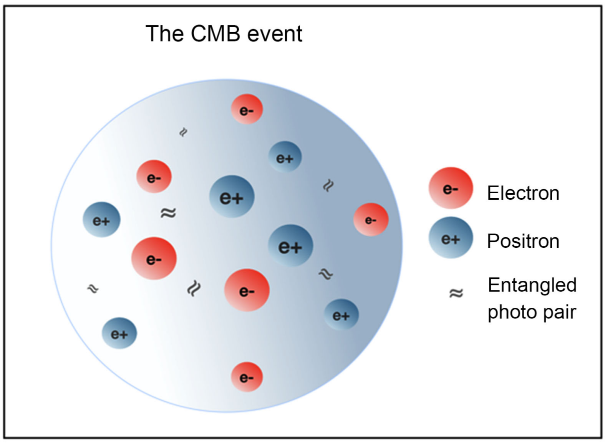

Figure 13. A schematic image of the primordial universe before the CMB transition event.

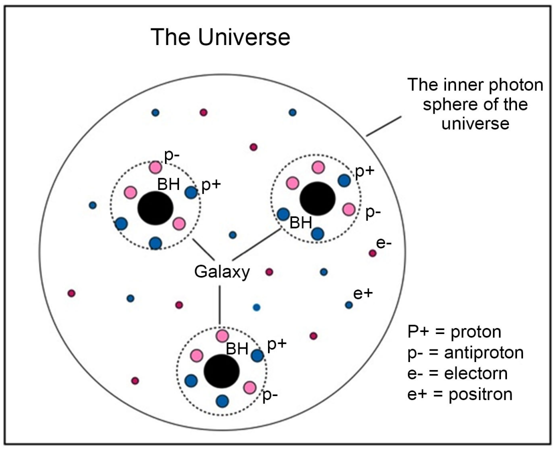

Figure 14. A schematic image of the universe after the CMB transition event.

This might sound as a strange hypothesis, but, as we will see, the numerical evidence is convincing. The standard model is incapable of explaining the current photon density. If all real energy was stored in photons at the time of the CMB, the number of photons would be 1.22×10^{84} and the density 490 ph/m^3, *i.e.* far from the previous number.

The expansion advances in all 3d directions, the number of photons increases according to

$$N'_{ph0} = \frac{N_{phc}}{a_c^3}. \tag{133}$$

When photons enter the observable universe with a scale factor of a_{fl} (first light), they so to speak, pass a single slit, a moment continuously changing with the expansion, only to be observed at the planet Earth in the Milky Way galaxy after about 14.0 Gyr. During the passage the relativistic Doppler effect, see Box below, increases the wavelength and thus lowers the photon energy. Since they are in superposition the compensation means an increase proportional to $1/a_{fl}$.

Currently the total number of CNB photons is

$$N_{ph0} = \frac{N_{phc}}{a_{fl} a_c^3}. \quad (134)$$

7.3.2. The Energy Density of the CMB

At the CMB transition, as hypothesized in Section 7.3.1, the energy splits into two components, the radiation from the CMB and the matter in the black holes. The following equation describes the transition:

$$r_{uc} = \frac{G_c W_{xc}}{c^4} + \frac{G_c M_{mc}}{c^2} \geq r_s = \frac{2G_c M_{mc}}{c^2}, \quad (135)$$

where G_c is the gravitational parameter, W_{xc} is the radiation energy and M_{mc} is the mass of all matter at a_c.

Box: Relativistic Doppler effect

The relativistic expansion velocity is a fraction v_{exp} of the speed of light, we have

$$v_{exp} = B\sqrt{L}. \quad (B1)$$

The increasing velocity causes a prolongation of the wavelength, the Doppler effect. The relativistic velocity difference is obtained from, cf. HyperPhysics/Relativistic Doppler,

$$v_{\Delta} = \frac{v_{exp0} + v_{exfl}}{1 + v_{exp0} v_{exfl}}. \quad (B2)$$

The scale factor a_{fl} is obtained from

$$a_{fl} = \sqrt{\frac{1 - v_{\Delta}}{1 + v_{\Delta}}}. \quad (B3)$$

The value obtained by iteration is $a_{fl} = 0.0173$, the same as in Figure 4.

At the transition we have

$$\frac{W_{xc}}{c^2} = M_{mc} = \frac{W_u(r_c)}{2c^2}. \quad (136)$$

The CMB energy is

$$W_{xc} = \frac{1}{2} W_u(r_c) = 2\pi b a_c^2 r_o^2 = 6.32 \times 10^{61}\ \text{J}. \quad (137)$$

The number of photons is

$$N_{phc} = \frac{W_{xc}}{W_e} = 7.72 \times 10^{74}. \quad (138)$$

The scale factor for the "first light" moment of the observable universe was determined in [6]: $a_{fl} = 0.0173$, a value resembling $t_{fl} = 0.261$ Gyr, which is in good conformity with estimates of today.

The total number of photons is, Equation (134),

$$N_{ph0} = \frac{N_{phc}}{a_{fl} a_c^3} = 1.024 \times 10^{90}.$$

The number density is

$$n_{ph0} = \frac{N_{ph0}}{V_0} = 410\times10^6\ \mathrm{m}^{-3}, \tag{139}$$

where $V_0 = 2.493 \times 10^{81}\ \mathrm{m}^3$. n_{ph0} is in good agreement with present data.

The energy density of the CMB is

$$w_{x0} = n_{ph0} W_{ph0} = 4.173\times10^{-14}\ \mathrm{J/m^3}. \tag{140}$$

The result is practically identical with the current Black Body density $w_{BB0} = \alpha_B T_0^4 = 4.175\times10^{-14}\ \mathrm{J/m^3}$, where $\alpha_B = 7.565723\times10^{-16}\ \mathrm{J}/\left(\mathrm{m^3\cdot K}\right)$ is the Boltzmann radiation density and $T_0 = 2.7548$ K.

8. Galaxies

8.1 The Galaxy Black Hole

The black holes in the centre of the galaxies are seeds stemming from the CMB transition. During the transition, half of the energy forms the CMB radiation, while the other half is spread out in 10^{12} - 10^{13} galaxy black holes. Right after the CMB event the total energy of the BHs is $W_{Bctot} = 0.5\times4\pi rbr_c^2 = 6.32\times10^{61}\ \mathrm{J}$. There are several indications that the radius r_B of an individual BH changes very slowly, which is also shown by the outcome of this study.

We use the inner photon radius R_B as the appropriate radius instead of the Schwarzschild radius $r_s = 2\cdot R_B$. We have

$$R_B = \frac{M_B G}{c^2}, \tag{141}$$

where M_B is the mass of the BH and G is the gravitation parameter of the universe at a given time. *With G inversely proportional to the scale factor a and R_B constant M_B becomes inversely proportional to a*, ($M_{B0} = M_{Bc}/a$). Currently the energy content of all black holes is:

$$W_{B0tot} = W_{Bctot}/a_c = 1.793\times10^{66}\ \mathrm{J} \quad \text{or} \quad M_{B0tot} = 2.00\times10^{49}\ \mathrm{kg} \quad (10^{19}\ \text{suns})$$

The estimates of the number of galaxies are so far very rough, a common number is 2×10^{11} for the observable universe or 1.6×10^{12} for the whole world, cf. Mario Livio, The Universe. Space. Tech., June 2022. The average BH mass would then be 1.25×10^{37} kg or 6×10^6 solar masses. These numbers are quite usual according to observations. The black hole of the Milky Way, Sagittarius* is estimated to have a mass of 8.3×10^{36} kg.

When G from Equation (15) is substituted into Equation (141) we have

$$M_B = \frac{2\pi b R_B r}{c^2}. \tag{142}$$

The mass of an individual BH increases at the same rate as the universe itself, *i.e.* inversely proportional to *a*. Like in the universe case there is an influx of electron-positron pairs.

The time derivative is

$$\frac{\mathrm{d}M_B}{\mathrm{d}t} = \frac{2\pi b R_B \sqrt{BL}}{c}. \tag{143}$$

The equation is needed later, when we want to determine the star formation change with time as a function of the galaxy's stellar mass, cf. **Figure 18**.

The black hole has an inside gravitational parameter (on the surface), by applying Equation (6) we have

$$G_B = \frac{c^4}{2\pi b R_B}. \tag{144}$$

The parameter contains only constants and is accordingly a constant itself.

8.2. Instead of a Singularity

In the current study, the universe is considered to be a black hole without a singularity. The reason lies in the pressures that cause the expansion and their opposite action against gravitational contraction. The curvature of space governs electron-positron influx and thereby regulates the pace of expansion. In the *galaxy BH*s we can equally define a balance equation between expansion and contraction. Compared to the *universe BH* there is a much more moderate influx of electron-positron pairs (see next section) that causes an increase in the density without increasing the size.

The pressure driving the density increase is obtained from

$$\frac{\mathrm{d}W}{\mathrm{d}t} + P\frac{\mathrm{d}V}{\mathrm{d}t} + V\frac{\mathrm{d}P}{\mathrm{d}t} = 0. \tag{145}$$

The volume is constant along with R_B, so we are left with the equation

$$\frac{\mathrm{d}W}{\mathrm{d}t} = -V\frac{\mathrm{d}P}{\mathrm{d}t}. \tag{146}$$

The expansion pressure is

$$P_{Bexp} = -\frac{W_B}{V_B} = -\frac{3br}{2R_B^2}, \tag{147}$$

where V_B is the volume of the black hole.

The acceleration directed outwards is

$$g_{Bexp} = \frac{4\pi G_B P_{exp}}{3c^2} = -\frac{rc^2}{R_B^2}. \tag{148}$$

Alternatively, the same result is obtained by considering that $g = -\nabla\phi$, where $\phi = -G_B M_B / R_B$. For the symmetric spherical case we have

$$g_{Bexp} = \frac{\partial}{\partial R_B}\left(\frac{rc^2}{R_B}\right) = -\frac{rc^2}{R_B^2}. \tag{149}$$

The contracting acceleration due to gravitation is obtained from the familiar equation

$$g_{Bcontr} = \frac{G_B M_B}{R_B^2} = \frac{rc^2}{R_B^2}. \tag{150}$$

We end up with the balance equation

$$g_{Bexp} + g_{Bcontr} = 0. \tag{151}$$

8.3. Influx of Baryonic Matter from the Black Hole

The black hole has two boundary spheres, the inner one or the photon sphere, $r_B = 0.5 \cdot r_s$ and the outer one or the black hole event horizon at r_s. In between there is an energy gap. From these boundaries there is an influx of electron-positron pairs into the inside of the BH and proton-antiproton pairs into the space outside the BH, Figure 15. In the *galaxy BH* case the number of injected pairs, N_{pair}, is equal on the inside as on the outside, because $\sqrt{R_B/R_B} = 1$.

According to our earlier stated postulate all stellar matter of a galaxy originates from the central BH event horizon. As a result we obtain a clear-cut relation between the stellar mass, M_S, and the BH mass, M_B. The relation is

$$\frac{M_S}{M_B} = \frac{2\nu_{Bi}^2 m_p N_{pair}}{2m_e N_{pair}} = \nu_{Bi}^2 \frac{m_p}{m_e} = 1786.4. \tag{152}$$

This is a significant result. Some bold presumptions lead to a result that has a strong anchorage in current observations. The average example of Section 8.1, $M_B = 1.25 \times 10^{37}$ kg, suggests a galaxy stellar content of 2.23×10^{40} kg, which is a typical value.

During the last decade several papers have been published, wherein the mass ratio is discussed and different theories about the cause has been presented, cf. [31] [32] and [33]. The standard theory suggests that stellar matter feeds the black holes, not vice versa as the present theory (CBU) suggests.

An indication that the CBU result is the most plausible one, is shown in Figure 16. The line $M_B = \left[\nu_{Bi}^2 \left(m_p/m_e\right)\right]^{-1} \cdot M_S$ is shown in a chart created by Sandra Faber, [34]. There is a perfect fit with the "Small dense" galaxies. The line shows there is a linear correlation, which for the present theory means that M_B grows linearly and the assumption of R_B being constant is correct.

In Figure 17, a similar pattern as in Figure 16 is shown for galaxes of type "Active Galactic Nucleus", [31] indicating that the ratio $M_S/M_B = \nu_{Bi}^2 \left(m_p/m_e\right)$ results in a perfect fit. In Figure 18 the change in stellar mass $\mathrm{d}M_S/\mathrm{d}t$ is shown as a function of the mass. Here the observations are related to galaxies in a star forming phase, cf. [35]. The CBU theoretical time derivative hits into the middle of the statistical pattern.

9. Total Energy

In the original CBU model it was assumed, that the total energy was proportional to the curvature radius r squared. However, the new understanding requires the addition of a term considering the energy generated by the g*alaxy BHs*. Notice, that this is not free energy, the negative counterpart is the gravitational potential energy provided by the increasing density of the black hole. The potential acts over the gap between R_s (event horizon, equal to the Schwarzschild radius) and R_B.

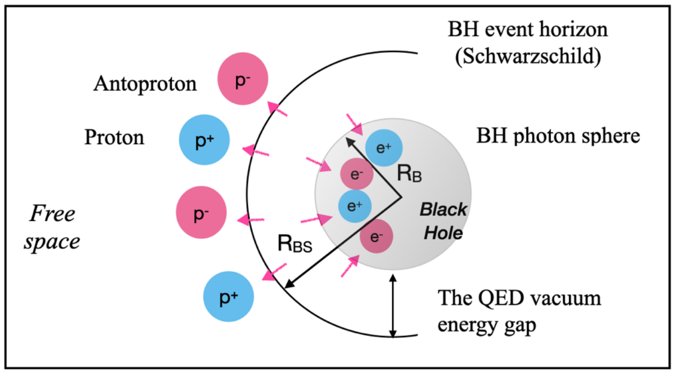

Figure 15. A schematic image of the influx of electron-positron pairs into the BH interior and proton-antiproton pairs into the BH surrounding.

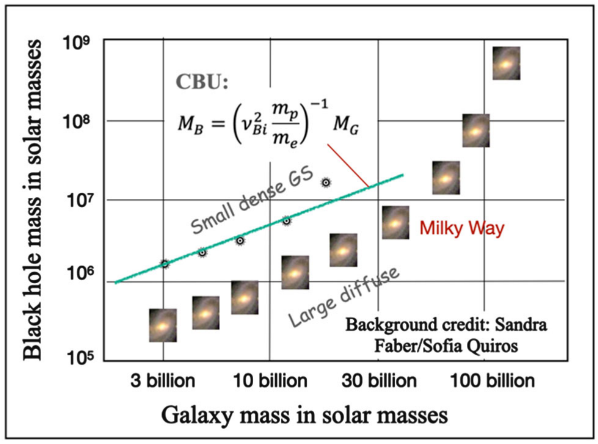

Figure 16. A wide-ranging publicly distributed chart showing the results of the relation $M_B = f(M_G)$ for numerous observed galaxies, [34]. (Here presumed that the galaxy mass M_G equals the stellar mass M_S.)

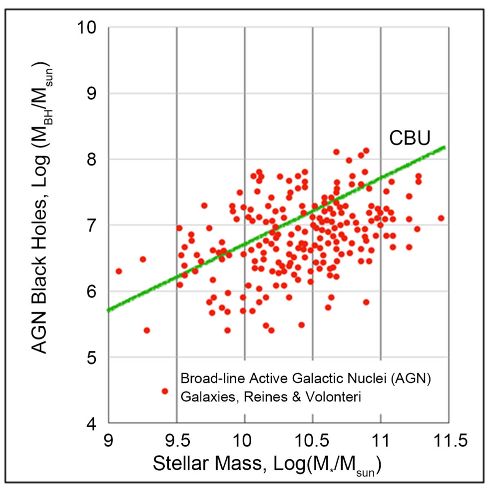

Figure 17. The CBU theory M_B-M_S relation (green line) shows good correlation with the observations of the Reines&Volonteri team, [31].

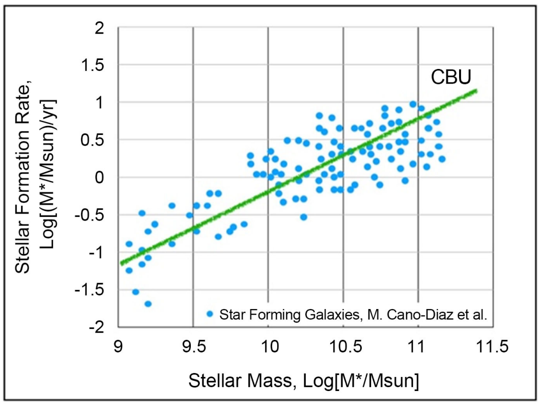

Figure 18. The time derivative of the stellar mass as a function of the mass (green line) according to the CBU theory shows good correlation with the observations of the Cano-Diaz team, [35]. ($M_S = M^*$).

The energy due to the electron-positron influx is

$$W_{ue^+e^-} = 4\pi br^2. \tag{153}$$

The total energy of the galaxies and the black holes is

$$W_G = W_{Su} + W_{Bu} = 2\pi br^2 a_c \left(v_{Bi}^2 \frac{m_p}{m_e} + 1 \right), \tag{154}$$

where W_{Su} and W_{Bu} are the overall energies of the stellar matter + dust + radiation and the black holes respectively.

The original estimate of the total energy (matter and radiation) was W_{u0} = 1.018×10^{71} J. The corrected value is $W_{u0tot} = 1.050 \times 10^{71}$ J. The increase due to the galaxies is 3.15%.

The critical density is

$$\rho_{cr} = \frac{3h_0^2}{8\pi G_0} = 8.72 \times 10^{-27} \frac{\text{kg}}{\text{m}^3}, \tag{155}$$

where $h_0 = 2.208 \times 10^{-18}$ 1/s and $G_0 = 6.67430 \times 10^{-11}$ m^3/kg/s^2. In the CBU model the critical density does not have a real meaning, because basically the universe grows eternally from the inside, there is no critical limit deciding whether the expansion will stop or continue for ever.

10. Theory Comparison, Arguments in Favour of the CBU Theory

A theory in natural sciences can only be tested by observations and measurements. In **Table 2** some of the most important characteristics of the CBU and ΛCDM theories are compared with each other. The numbers are in good agreement, especially considering the different approaches. The main discrepancies relate to the interpretation of the energy content. In the standard model dark energy and dark matter are considered real, while in the CBU dark energy is a virtual ingredient, the vacuum energy from which the universe, in accordance

Table 2. CBU versus ΛCDM.

Characteristic	*CBU*	*ΛCDM*, [17]	*Diffr. %*
Radius of the obs. universe, 10^{26} m	4.206	4.396	+4.5
Age of the universe, 10^9 y	14.45	13.797	−4.7
Hubble parameter, 10^3 m/s/Mpc	68.1	67.7	−0.6
Matter + rad. density parameter, Ω_{mx}	0.05374	0.0498	−5.9
Dark energy density parameter, Ω	0.723	0.686	−5.4
Total real energy, 10^{71} J (matter + radiation)	1.050	1. 079	+2.7
CBU: Free space, 10^{71} J	1.018		
CBU: Black holes, 10^{71} J	0.000018		
CBU: Galaxies, 10^{71} J	0.0320		

with the uncertainty principle, picks up particles that accumulate as real energy. However, the virtual vacuum energy does not lead to an accumulation. Further, the CBU does not require dark matter to explain galaxy dynamics.

The CBU theory has uncovered several characteristics of the universe that seem hard to accept as coincidences. Here are the most essential ones:

1) The radius of the observable universe $r_0 = 4.206 \times 10^{26}$ m derived from the assumption that the universe is a black hole, the standard model value is 4.396×10^{26} m.

2) The ratio of the electron rest energy ($m_e c^2$) and the radius of the maiden universe (r_i) defines an energy constant b, Equation (14), that times the square of the radius r of the observable universe results in a real energy value in complete conformity with current estimates: the r^2 law, also predicted by the Dirac Large Number Hypothesis.

3) The Schrödinger solution to the virgin universe leads to an exponential constant equal to the Planck length given the Newtonian gravitational constant G is a parameter dependent on the curvature radius r.

4) The Planck length ℓ_{Pi} divided by the curvature diameter of the virgin universe, $2r_i$, equals a number consisting of fundamental constants, cf. Equation (67):

$$\frac{\ell_{Pi}}{2r_i} = \sqrt{\frac{2\pi - 1}{4\alpha_{fs}}} = 13.4535,$$

where α_{fs} is the fine structure constant. The numeral equals the ratio between virtual dark energy and total real energy, $\Omega_\Lambda/\Omega_{mx}$ (Ω_{mx} equals the standard model $\Omega_b + \Omega_r$).

5) The introduction of an acceleration factor B results into density and pressure expressions that provide a consistent solution to the Einstein Field Equation

$$G_{\mu\nu} = T_{\mu\nu}.$$

6) The hypothesis that the vacuum gap between the event horizon and the inner photon sphere of a black hole causes the excitation of electron-positron pairs

on the inside and proton-antiproton pairs on the outside of the BH is best proved correct by the graphs of **Figures 16-18**. The magnitude and slope of the theoretical curves follow accurately the statistical average of observational data.

11. Conclusions

Theories about the universe are based on hypotheses and educated guesses. Observations and sceptical criticality are the only tools to approach the truth. At the core of the standard model there are five central hypotheses: the Big Bang itself, inflationary expansion, dark energy, dark matter and last scattering as the CMB explanation.

In this study, we try to keep the hypotheses to a minimum and as close to known laws of physics as possible. However, there are assumptions that require scientific confirmation. Such are the black hole universe, the influx of matter from the black hole boundary spheres and the propagation of entangled photons in a superposition.

Even if the CBU theory in principle follows a plausible track, it is not perfect, many details need deeper penetration. One such area is how protons and antiprotons transforms into neutrons, electrons, neutrinos and further into atoms. The problem is similar to that of nucleosynthesis in the primordial universe of the standard model.

It is our hope that the propositions presented here will lead to new insight in the world of quantum mechanics and the understanding of the connection between gravity and the quantum world.

Conflicts of Interest

The author declares no conflicts of interest regarding the publication of this paper.

References

[1] Lemaitre, G. (1931) *Nature*, **127**, 706. https://doi.org/10.1038/127706b0

[2] Guth, A. (1997) The Inflationary Universe: The Quest for a New Theory of Cosmic Origins. Perseus Books, New York. https://doi.org/10.1063/1.881979

[3] Hubble, E. (1929) *Proceedings National Academy of Science* (*USA*), **15**, 168-173. https://doi.org/10.1073/pnas.15.3.168

[4] Einstein, A. (1916) *Annalen der Physik*, **49**, 769-822. https://doi.org/10.1002/andp.19163540702

[5] Einstein, A. (1917) Kosmologische Betrachtungen zur allgemeinen Relativitätstheorie. Sitzungsberichte der Preussischen Akad. d. Wissenschaften.

[6] Eriksson, J.-T. (2018) *International Journal of Physics*, **6**, 38-46.

[7] Eriksson, J.-T. (2019) *International Journal of Physics*, **7**, 16-20. https://doi.org/10.12691/ijp-7-1-3

[8] Eriksson, J.-T. (2021) *International Journal of Physics*, **9**, 240-244. https://doi.org/10.12691/ijp-9-5-3

[9] Eriksson, J.-T. (2020) *International Journal of Physics*, **8**, 64-70.

[10] Eriksson, J.-T. (2021) *International Journal of Physics*, **9**, 169-177. https://doi.org/10.12691/ijp-9-3-4

[11] Eriksson, J.-T. (2022) *International Journal of Physics*, **10**, 144-153. https://doi.org/10.12691/ijp-10-3-3

[12] Pathria, R.K. (1972) *Nature*, **240**, 298-299. https://doi.org/10.1038/240298a0

[13] McBryan, B. (2013) Living in a Low-Density Black Hole.

[14] Brans, C. and Dicke, R.H. (1961) *Physical Review*, **124**, 925-935. https://doi.org/10.1103/PhysRev.124.925

[15] Dirac, P.A.M. (1974) *Proceedings of the Royal Society of London. Series A*, **338**, 439-446. https://doi.org/10.1098/rspa.1974.0095

[16] Perlmutter, S. (2003) *Physics Today*, **56**, 53. https://doi.org/10.1063/1.1580050

[17] Carrol, S. (1997) Lecture Notes on General Relativity. University of Chicago, Chicago.

[18] Davis, T. and Lineweaver, C.H. (2003) Expanding Confusion: Common Misconceptions of Cosmological Horizons and the Superluminal Expansion of the Universe.

[19] Crighton, N. (2015) Make a Plot with both Redshift and Universe Age Axes Using astropy.cosmology. Ipython.display. Cosmological Calculations.

[20] McGaugh, S.S. and Lelli, F. (2016) *Physical Review Letters*, **117**, Article ID: 201101. https://doi.org/10.1103/PhysRevLett.117.201101

[21] Lelli, F., McGaugh, S.S., Schombert, J.M. and Pawlowski, M.S. (2016) *The Astrophysical Journal*, **836**, 152. https://doi.org/10.3847/1538-4357/836/2/152

[22] Milgrom, M. (2014) *Canadian Journal of Physics*, **93**, 107-118. https://doi.org/10.1139/cjp-2014-0211

[23] Eadie, M.G., Springford, A. and Harris, W.E. (2016) Bayesian Mass Estimates of the Milky Way.

[24] Salucci, P. (2017) Dark Matter Strikes Back.

[25] LAMOST Survey (2016) The Milky Way's Rotation Curve out to 100 kpc and Its Constraint on the Galactic Mass Distribution, Press Release November 18, 2016.

[26] BigThinc (2018, Oct. 31).

[27] Adler, R.J. (2010) *American Journal of Physics*, **78**, 925-932. https://doi.org/10.1119/1.3439650

[28] Huchra, J. (2018) Extragalactic Redshifts, NED, NASA/IPAC Extragalactic Database.

[29] Ringermacher, H.I. and Mead, L.R. (2015) *The Astronomical Journal*, **149**, 137. https://doi.org/10.1088/0004-6256/149/4/137

[30] Nemiroff, R. and Bonnell, J. (2013) Astronomy Picture of the Day, APOD.NASA, April 8, 2013.

[31] Reines, A.E. and Volonteri, M. (2015) *The Astrophysical Journal*, **813**, 82.

[32] Chen, Z., Faber, S.M., *et al.* (2020) *The Astrophysics Journal*, **897**, 102.

[33] Taerrazas, B.A., Bell, E.F., Pillepich, A., *et al.* (2020) *Monthly Notices of the Royal Astronomical Society, MNRAS*, **493**, 1888-1906. https://doi.org/10.1093/mnras/staa374

[34] SciTechDaily (2020) How Galaxies Die: New Insight into Galaxy Halos, Black Holes, and Quenching of Star Formation. University of California Santa Cruz, Santa Cruz.

[35] Cano-Diaz, M., *et al.* (2016) *The Astrophysical Journal Letters*, **821**, L26. https://doi.org/10.3847/2041-8205/821/2/L26